UCLA
UCLA Previously Published Works

Title

Precision modulation of dysbiotic adult microbiomes with a human-milk-derived synbiotic reshapes gut microbial composition and metabolites

Permalink

Journal

ISSN

Authors

Button, Julie E
Cosetta, Casey M
Reens, Abigail L
et al.

Publication Date

DOI
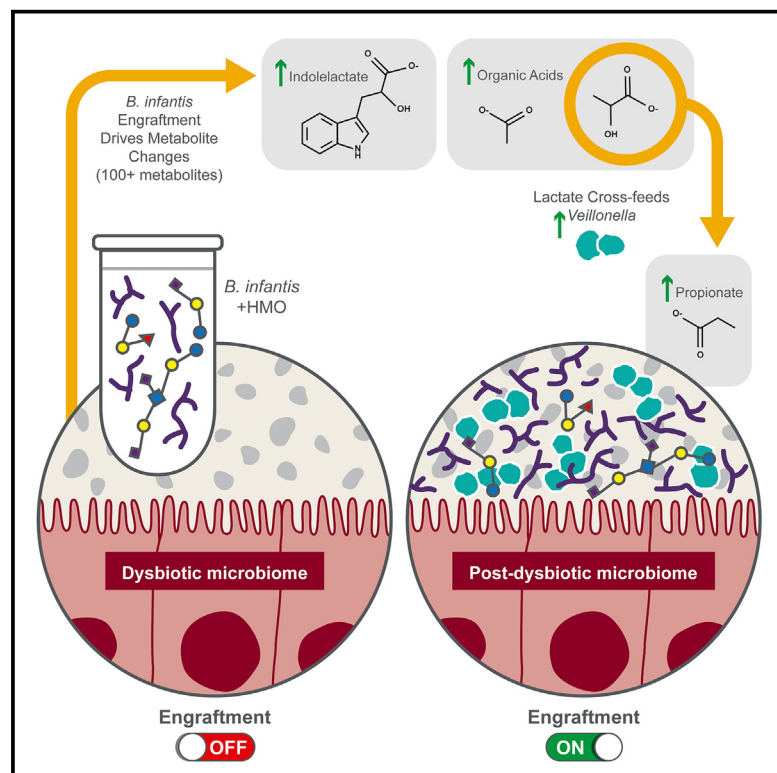
Peer reviewed

Cell Host & Microbe

Precision modulation of dysbiotic adult microbiomes with a human-milk-derived synbiotic reshapes gut microbial composition and metabolites

Graphical abstract

Authors

Julie E. Button, Casey M. Cosetta, Abigail L. Reens, ..., David J. Rechtman, Robert R. Jenq, Gregory J. McKenzie

Correspondence

gmckenzie@prolacta.com

In brief

Button et al. demonstrate precision microbiome engineering through human-milk-oligosaccharide-fed *Bifidobacterium longum* subspecies *infantis* in adult, antibiotic-perturbed gut microbiomes. Engraftment in adult subjects leads to reproducible changes in the microbiome, including cross-feeding of propionate-producing *Veillonella* spp. Reproducible positive impacts on an array of microbial metabolites point to therapeutic potential.

Highlights

- *B. infantis* engrafts into an antibiotic-perturbed adult human gut microbiome

- HMOs support engraftment of *B. infantis* in adults at up to 81% relative abundance

- Microbiome structure and gut metabolite levels were altered in engrafted adults

- *B. infantis* cross-fed *Veillonella* in adult patients, mouse models, and *in vitro*

CellPress

Cell Host & Microbe

CellPress

Clinical and Translational Report

Precision modulation of dysbiotic adult microbiomes with a human-milk-derived synbiotic reshapes gut microbial composition and metabolites

Julie E. Button,[1] Casey M. Cosetta,[1] Abigail L. Reens,[1] Sarah L. Brooker,[1] Aislinn D. Rowan-Nash,[1] Richard C. Lavin,[1] Russell Saur,[1] Shuning Zheng,[1] Chloe A. Autran,[1] Martin L. Lee,[1,2] Adam K. Sun,[1] Amin M. Alousi,[3] Christine B. Peterson,[4] Andrew Y. Koh,[5,6,7] David J. Rechtman,[1] Robert R. Jenq,[8] and Gregory J. McKenzie[1,9,*]
[1]Prolacta Bioscience, Duarte, CA 91010, USA
[2]Department of Biostatistics, University of California Los Angeles, Fielding School of Public Health, Los Angeles, CA 90095, USA
[3]Department of Stem Cell Transplantation, Division of Cancer Medicine, The University of Texas M. D. Anderson Cancer Center, Houston, TX 77030, USA
[4]Department of Biostatistics, The University of Texas M.D. Anderson Cancer Center, Houston, TX 77030, USA
[5]Department of Pediatrics, Division of Hematology/Oncology, The University of Texas Southwestern Medical Center, Dallas, TX 75235, USA
[6]Harold C. Simmons Comprehensive Cancer Center, The University of Texas Southwestern Medical Center, Dallas, TX 75390, USA
[7]Department of Microbiology, The University of Texas Southwestern Medical Center, Dallas, TX 75390, USA
[8]Department of Genomic Medicine, Division of Cancer Medicine, The University of Texas M.D. Anderson Cancer Center, Houston, TX 77030, USA
[9]Lead contact
*Correspondence: gmckenzie@prolacta.com
https://doi.org/10.1016/j.chom.2023.08.004

SUMMARY

Manipulation of the gut microbiome using live biotherapeutic products shows promise for clinical applications but remains challenging to achieve. Here, we induced dysbiosis in 56 healthy volunteers using antibiotics to test a synbiotic comprising the infant gut microbe, *Bifidobacterium longum* subspecies *infantis* (*B. infantis*), and human milk oligosaccharides (HMOs). *B. infantis* engrafted in 76% of subjects in an HMO-dependent manner, reaching a relative abundance of up to 81%. Changes in microbiome composition and gut metabolites reflect altered recovery of engrafted subjects compared with controls. Engraftment associates with increases in lactate-consuming *Veillonella*, faster acetate recovery, and changes in indolelactate and p-cresol sulfate, metabolites that impact host inflammatory status. Furthermore, *Veillonella* co-cultured *in vitro* and *in vivo* with *B. infantis* and HMO converts lactate produced by *B. infantis* to propionate, an important mediator of host physiology. These results suggest that the synbiotic reproducibly and predictably modulates recovery of a dysbiotic microbiome.

INTRODUCTION

The microbiota of the human gastrointestinal tract comprises a complex community that plays an important role in the maintenance of health and resistance to disease.[1,2] A multitude of factors, including host diet, environmental exposures, and antibiotic (Abx) usage influence the composition of the microbiome, sometimes leading to dysbiosis and negative health consequences. One promising approach to treat or prevent disease is via direct manipulation of the dysbiotic microbiome. Clinical success has been achieved for applications such as minimizing the recurrence of *Clostridioides difficile* infection.[3,4] These therapies, termed live biotherapeutic products (LBPs), may "engraft," or durably persist, in the recipient gastrointestinal tract and thereby lead to positive outcomes.[5,6] LBPs are under investigation for the treatment of a wide variety of diseases, spanning infectious, inflammatory, and metabolic diseases, but control of their engraft-

ment, accurate prediction of their efficacy, and effects on co-resident microbes and their metabolic pathways have not yet been demonstrated.[7–12] Not only is selection of microbial species a challenge, but questions remain about persistence and function within the recipient microbiome.[13–20]

A synbiotic pairing of a microbe and its preferred nutrient source, a prebiotic, increases the chance of engraftment by providing the LBP with a competitive advantage within the gut environment.[21–23] We previously described successful engraftment in healthy adults treated with a synbiotic product that consisted of *Bifidobacterium longum* subspecies *infantis* (*B. infantis*) as the LBP and a concentrate of human milk oligosaccharides (HMOs) as the prebiotic.[24] HMO are a structurally diverse class of oligosaccharides unique to human milk that consist of at least one lactose residue linked to various combinations of fucose, sialic acid, N-acetylglucosamine, or lacto-*N*-biose.[25,26] HMO are indigestible by humans and therefore available to gut

microbes, especially *Bifidobacterium* spp.[27–30] *B. infantis*, which is typically only found in the gut of breastfed infants, encodes clusters of HMO-utilization genes that enable it to efficiently import and metabolize the full spectrum of HMO molecules present in human milk.[31,32] Moreover, capacity for intracellular degradation of HMO provides *B. infantis* with an exclusive advantage over other species in the community.[33] Lactate and acetate are both produced during HMO degradation, and these organic acids are then either absorbed by the host or utilized by other members of the microbiota. Lactate and acetate cross-feed other microbes, resulting in the subsequent production of other short-chain fatty acids (SCFAs) like butyrate.[34–40] SCFAs are normally present in the lower gastrointestinal tract at ~100 mM and influence host physiology in multiple ways, including promotion of gut barrier function and immune tolerance.[41–45] By impacting microbes and metabolites, *B. infantis* has the potential to be an important modulator of gut health. Indeed, engraftment of *B. infantis* into the immature, low-diversity microbiome of breastfed babies leads to measurable beneficial results, including a reduction in the pathobiont-containing taxon *Enterobacteriaceae*, a reduction in detectable virulence genes, increases in levels of organic acids in fecal samples, and modulation of intestinal immunity.[46–48]

Previously, we observed engraftment of *B. infantis* into the microbiome of healthy adults and altered metabolite levels when *B. infantis* and HMO were both provided, but not in control cohorts provided with only HMO or *B. infantis*. HMO-dependent *B. infantis* engraftment occurred in ~60% of subjects at an average relative abundance of 5% and a maximum of 25%.[24] Significant changes in gut metabolites occurred, but there were few consistent changes in microbiome composition besides the expected increases in bifidobacteria.[24] HMO-dependent engraftment of *B. infantis* into unperturbed, colonization-resistant human microbiomes represents a powerful demonstration of a specific glycan promoting expansion of a bacterial taxon equipped to utilize that resource.[23] However, the context of a healthy, intact microbiome limits the ability to measure changes impactful in patient populations. Therefore, the next step was to assess the impact of the synbiotic in the context of microbiome dysbiosis.

To evaluate the effect of the synbiotic product in a perturbed microbiome, we induced dysbiosis by dosing healthy subjects with Abx, together with *B. infantis* and HMO, and measured recovery of microbiome composition and function. For comparison, we included a control cohort that did not receive HMO to assess *B. infantis* engraftment when the prebiotic is not provided. Abx-induced dysbiosis leads to lowered resistance to colonization by new microbial taxa and thereby likely enhances engraftment of LBPs.[5,49,50] In healthy adults, the acute disruption that occurs during and immediately following Abx is characterized by decreased diversity and altered levels of microbially produced metabolites. This period of severe dysbiosis is typically transient and limited to days or weeks, but some taxa may remain depleted for months to a year.[51–55] This may reflect long-term damage to the community or may simply represent a transition to a different but functionally equivalent stable state.[56] Transient dysbiosis may or may not be distinct from persistent, profound dysbioses, which require intervention to avoid disease. Persistent dysbiosis may be caused by prolonged or repeated treatment with Abx[57] or chemotherapeutics,[58] poor diet,[59] or ge-

netic and inflammatory factors.[60] In this study, we found that the administration of a synbiotic that consisted of *B. infantis* and HMO during and after Abx-induced dysbiosis resulted in significant changes in gut metabolites and microbiome composition, including high prevalence and abundance of engrafted *B. infantis*, together indicating that the trajectory of microbiome recovery had been altered. *B. infantis* and HMO reproducibly increased levels of lactate-consuming *Veillonella* spp. in humans and stimulated the production of the SCFA propionate by *Veillonella* when grown together, both *in vitro* and *in vivo*. The alterations to gut metabolites resulting from our treatment included faster recovery of fecal acetate levels, increased levels of lactate and indolelactate (ILA), and decreased levels of the pro-inflammatory metabolite p-cresol sulfate (pCS), all of which can impact host physiology. These data predict robust HMO-dependent engraftment of *B. infantis* into dysbiotic patient microbiomes with the potential to produce positive changes in microbiome composition and function.

RESULTS

High-level, HMO-dependent engraftment of *B. infantis* in healthy subjects after Abx exposure

We hypothesized that introduction of *B. infantis* and HMO into a microbiome disrupted by Abx would result in a high rate and level of engraftment and would serve as a good model to test the predicted positive effects of *B. infantis* on microbiome recovery. The study design included healthy human subjects co-treated with two different Abx: vancomycin, which primarily affects Gram-positive bacteria, and metronidazole, which affects anaerobes, including Gram-negative bacteria. Used together, these Abx broadly impact the gut microbial community.[61,62]

A total of 56 subjects were assigned to three different cohorts. Analyses of age, body mass index (BMI), sex, ethnicity, and race revealed no statistically significant differences between cohorts (Table S1). All cohorts received Abx, and the two test cohorts also received *B. infantis* or *B. infantis* with HMO (Figure 1). All subjects were followed through day 35, 1 week after all dosing ceased. No serious adverse events were observed in any subject, and all events are listed in Table S2.

B. infantis abundance was measured in stool samples using a qPCR assay (Figure 2A). For subjects who received Abx only (no *B. infantis*), levels remained below or near the limit of detection (LOD). For the two cohorts that received *B. infantis*, the low levels detected during Abx dosing were interpreted as "pass-through" due to Abx sensitivity (*in vitro* minimum inhibitory concentrations: vancomycin ≤ 0.5 μg/mL; metronidazole 8 μg/mL). After the cessation of Abx and with continued *B. infantis* dosing, levels rose in both *B. infantis*-treated cohorts above pass-through by day 11. On days 21 and 28, a significant difference was observed between the two *B. infantis* cohorts (Sidak's post test, p_{adj} = 0.003 and p_{adj} = 0.002, respectively) and over time (mixed effects model, $p < 0.0001$). Subjects without HMO exhibited a steady decline after dosing ceased, while most subjects given HMO displayed stable, high levels of *B. infantis* through day 28. Levels declined rapidly after HMO dosing ceased. Together, these data demonstrate that while Abx may temporarily reduce colonization resistance to enable transient expansion of *B. infantis*, co-dosing with HMO is essential for durable, high-level engraftment.
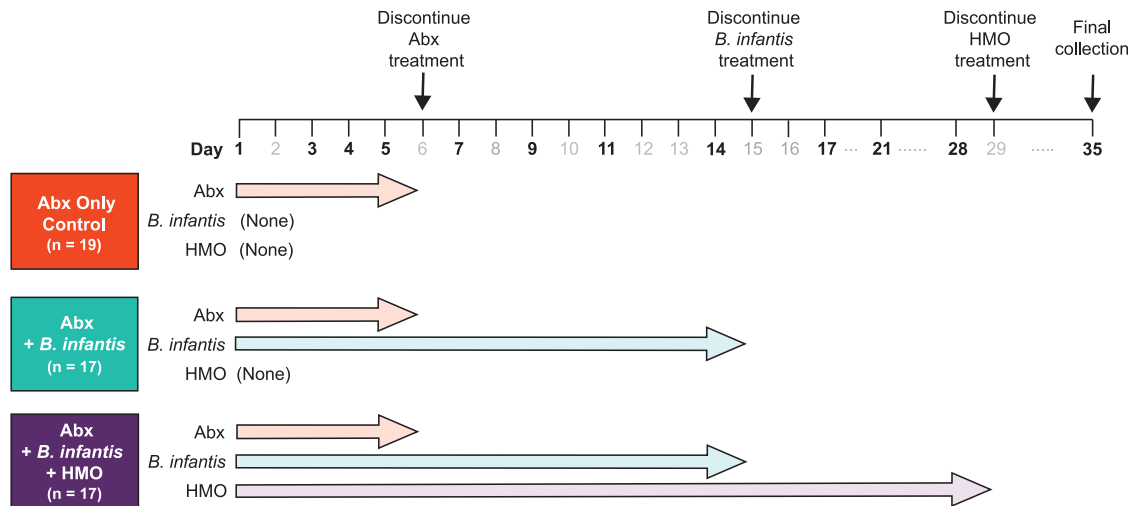
Cell Host & Microbe
Clinical and Translational Report

Figure 1. Healthy human subject study design
A schematic of the study design with 56 healthy participants assigned to 3 cohorts. Antibiotics (Abx) only: a 5-day course of vancomycin (250 mg dose/3 times per day) and metronidazole (500 mg dose/3 times per day) on days 1–5. Antibiotics and *B. infantis*: the same course of antibiotics with *B. infantis* ($\geq 8 \times 10^9$ colony-forming unit [CFU]/dose once per day) on days 1–14. Antibiotics, *B. infantis*, and HMO: the same course of antibiotics with *B. infantis* and with HMO (9 g twice daily for a total of 18 g/day) on days 1–28. Stool collection days are indicated in bold text. See also Tables S1 and S2.

In both cohorts dosed with *B. infantis*, there was evidence of two subpopulations: "engrafted," for which *B. infantis* was consistently maintained through day 28, and "not engrafted" (NE), where *B. infantis* was not consistently maintained (Figures 2B and 2C). Of subjects who received *B. infantis* + HMO, 76% (13/17) were deemed engrafted (Figure 2B). The four subjects defined as NE each produced at least one stool sample with no detectable *B. infantis* during dosing, suggesting possible non-compliance. *B. infantis* levels in engrafted subjects were significantly higher than in NE subjects over time (mixed effects model, p < 0.0001). The mean level of *B. infantis* at day 14 in engrafted subjects was ~5-fold higher than the overall mean of the cohort. Moreover, when only engrafted subjects within the *B. infantis* + HMO cohort were compared with the *B. infantis*-only control, levels were significantly higher as early as day 11 (Figure S1A; mixed effects model, p < 0.0001; Sidak's post test, p_{adj} < 0.0005).

Engraftment was also observed in four subjects who received *B. infantis* alone (without HMO), representing ~24% (4/17) of the cohort (Figure 2C). *B. infantis* levels in these subjects were ~100-fold lower than for engrafted subjects who received HMO. The rate of engraftment also differed significantly between the two cohorts (13/17 engrafted vs. 4/17 engrafted; Fisher's exact test, p = 0.0053). Our previous study in healthy adults with unperturbed microbiomes showed no evidence of engraftment without co-dosing with HMO.[24] Here, Abx exposure likely lowers colonization resistance.

Interestingly, some engrafted subjects from both cohorts retained *B. infantis* signal at day 35 (Figures 2B and 2C) To follow up, we collected additional stool samples from available subjects on or after day 90 (Table S3). *B. infantis* was below the LOD for nine subjects from the *B. infantis* + HMO cohort. For three subjects from the *B. infantis* (without HMO) cohort, levels were either low or undetectable (Table S3). These data suggest that in most subjects, *B. infantis* did not durably engraft without continued HMO treatment.

We next used whole metagenomic sequencing (WMS) of stool samples and a strain-specific tracking algorithm to quantify the relative abundance of *B. infantis* in the microbiome of each cohort. For engrafted subjects that received HMO, the median abundance over days 14–28 was 45.9%, with a maximum of 81% in one subject at day 9 (Figures 2D and S1B). Abundance was significantly lower over time in engrafted subjects that did not receive HMO, ranging from 0.7%–7.8% with a median of 3.4% (mixed effects model, p_{adj} = 0.0003). Using an orthogonal method with different sequence biases, we also calculated the ratio of *B. infantis* to total bacterial (16S) qPCR signal (Figures S1C and S1D). The results of this method were similar, with median relative abundance of engrafted subjects in the *B. infantis* + HMO cohort at 8.6% and a maximum of 48.4% during days 14–28.

Our previous study utilized the same methodology to measure engraftment in non-Abx-treated healthy adults.[24] A direct comparison of *B. infantis* abundance across both studies at days 14–15 in subjects receiving both *B. infantis* and HMO showed significantly higher levels in subjects with Abx-induced dysbiosis (Figure S1E; Sidak's post test, p_{adj} < 0.0001). This controllable, high-level engraftment maximizes the likelihood of positively impacting the gut microbiome. For this reason, analyses comparing the engrafted subset of subjects in the *B. infantis* + HMO cohort to the Abx-only control are most relevant for measuring impacts of high-level engraftment on the microbiome and gut metabolites.

HMO-mediated engraftment of *B. infantis* alters microbiome communities after transient, Abx-induced dysbiosis in healthy subjects, leading to a reproducible enrichment of *Veillonella*

Initially, WMS data from all subjects was evaluated for changes in microbial community composition. As expected, Abx induced transient, acute dysbiosis in all three cohorts. From days 1 (baseline) through 5 (end of Abx dosing), there were robust decreases in microbial diversity and a consistent shift in community
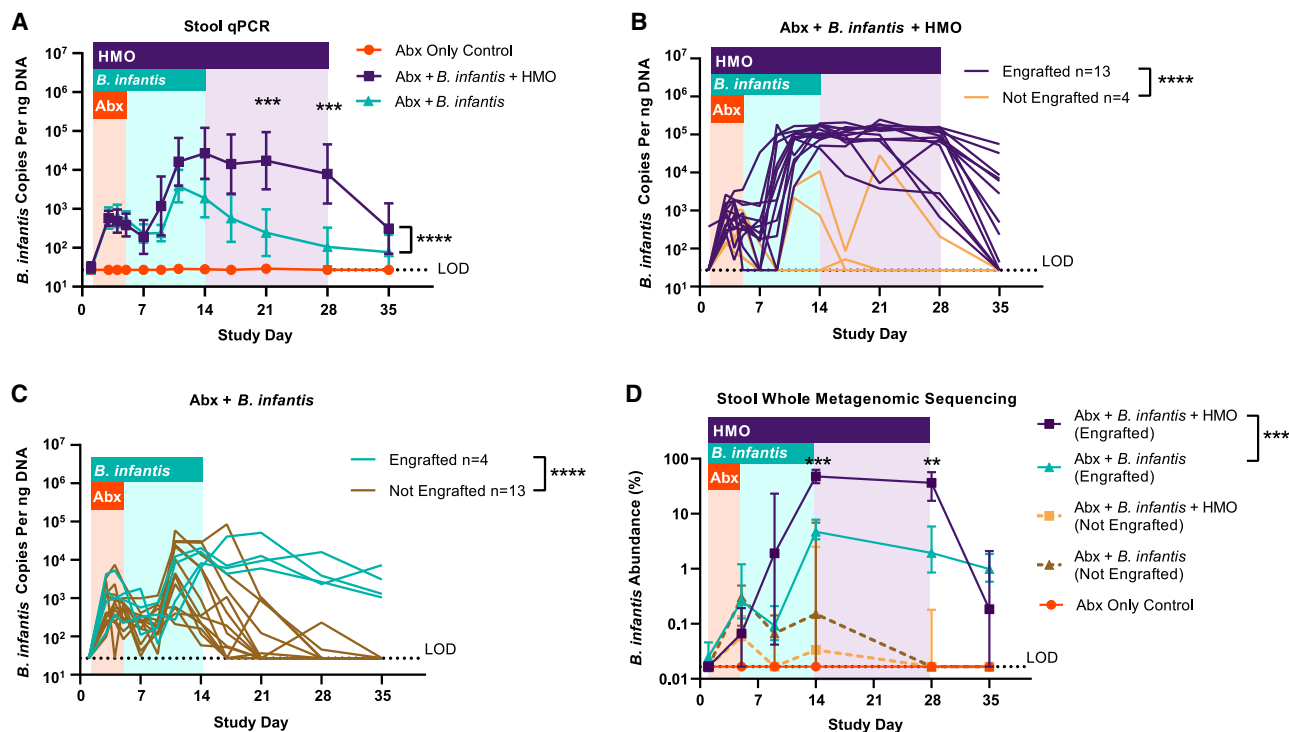
Figure 2. Perturbation of healthy microbiomes with Abx led to consistently high levels of *B. infantis* engraftment in subjects co-treated with HMO

(A) *B. infantis* abundance in stool samples was determined by qPCR and plotted as the average for all subjects in each cohort. Data are geometric means (Abx only, n = 19; *B. infantis* + HMO, n = 17; *B. infantis* only, n = 17) with 95% confidence intervals. The dotted line represents the limit of detection (LOD), 27 copies/ng DNA. Significance at individual time points and over time was determined for *B. infantis* + HMO vs. *B. infantis* only.

(B and C) Data for the indicated cohorts from (A) were replotted to separate engrafted from non-engrafted subjects. Subjects were deemed engrafted if *B. infantis* signal for two consecutive time points was two geometric standard deviations above the pass-through level (geometric mean of signal for all subjects dosed with *B. infantis* on days 3–5; equivalent to 5.4×10^3 copies/ng DNA). Traces represent individual subjects.

(D) *B. infantis* abundance in stool samples was determined by whole metagenome sequencing (WMS) using a strain-tracking algorithm. Each point represents the median of the indicated cohort subpopulation, and error bars represent the interquartile range. Undetected values were imputed with the LOD (lowest detected value). Significance at individual time points and over time were determined for *B. infantis* + HMO (engrafted) vs. *B. infantis* only (engrafted).

See also Figure S1 and Table S3.

composition (Figures 3 and S2A–S2C). Shannon diversity was significantly decreased in both cohorts by day 5 (Figure 3A; Sidak's post test, $p_{adj} < 0.0001$). Total bacterial abundance also decreased (Figure S2B), and microbiome community structure (Bray-Curtis dissimilarity) was significantly different by day 5 (Figure 3B; Table S4; PERMANOVA, $p_{adj} < 0.001$). Notably, levels of *Lactobacillaceae* and *Enterobacteriaceae* increased from ≤0.2% of the population to >76% and >16%, respectively (Figures 3C and S2C).

From days 5 to 35, all measures of microbiome diversity rebounded in all three cohorts. Shannon diversity increased by day 35 but remained significantly different from day 1 levels, suggesting that recovery was incomplete (Figure 3A; Sidak's post test, $p_{adj} < 0.01$). Similarly, while community composition trended toward day 1 measures, it remained distinct from this baseline in all cohorts at all post-Abx time points, suggesting incomplete recovery or recovery to an alternate stable state (Figure 3B; Table S4; PERMANOVA, $p_{adj} < 0.001$). Levels of *Lactobacillaceae* and *Enterobacteriaceae* decreased during the post-Abx period; conversely, bacteria characteristic of a healthy human microbiome, such as *Lachnospiraceae* and *Bacteroidaceae*,[63] increased in all cohorts by day 28 (Figures 3C and S2C).

Measures of alpha diversity suggested a reduction in diversity in the *B. infantis* + HMO cohort compared with the two control cohorts (Figures 3A and S2A), although total bacterial abundance did not differ (Figure S2B). Microbiome composition differed significantly between all subjects in the *B. infantis* + HMO and the control cohorts at day 14 (Figure S2D; PERMANOVA $p_{adj} < 0.01$). Engrafted subjects differed from Abx-only controls on both days 14 and 28 (Table S4; PERMANOVA, $p_{adj} < 0.001$). The abundant *B. infantis* in engrafted subjects at these time points could have explained the differences, however, we predicted changes in the underlying community as well. To address this, we subtracted reads corresponding to the genus *Bifidobacterium* using an approach similar to that used by the American Gut Project to exclude data from microbial blooms during sample storage.[64] With *Bifidobacterium* excluded, there were indeed significant differences in community structure between engrafted subjects receiving *B. infantis* + HMO and the Abx-only control (Figure 3D; Table S4; PERMANOVA, $p_{adj} < 0.001$). Furthermore, by measuring the distance between each point and the centroid within a cohort, there was significantly less Bray-Curtis dissimilarity among individual engrafted subjects within the *B. infantis* + HMO cohort compared with the

Cell Host & Microbe
Clinical and Translational Report

CellPress
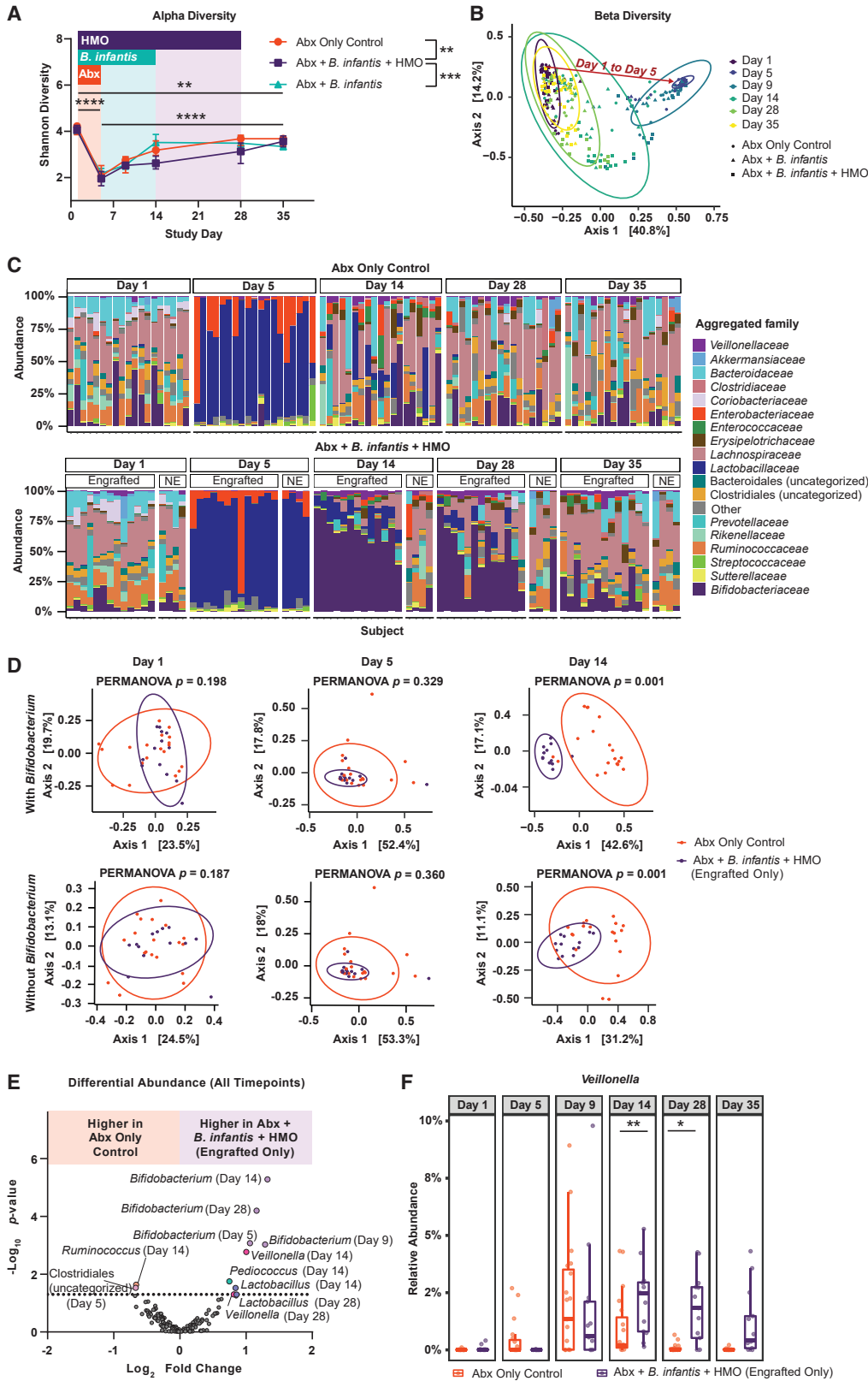
Abx cohort at day 14, regardless of the inclusion of *Bifidobacterium* reads (Figure 3D; ANOVA, $p_{adj} < 0.05$). This suggests that engraftment of *B. infantis* after Abx may have steered microbiome recovery toward a more consistent community structure.

We next compared abundance of specific taxa, again between engrafted subjects who received *B. infantis* + HMO and the Abx-only cohort. Besides the expected increase in *Bifidobacterium* at various time points, *Lactobacillus* and *Veillonella* were significantly higher in the *B. infantis* + HMO engrafted subset at days 14 and 28, as was *Pediococcus* at day 14 (Figures 3E, 3F, S3B, S3D, S3F, S3H, and S3J; Wilcoxon's rank sum test, all $p_{adj} < 0.05$). *Veillonella* abundance was <0.05% at day 1 and increased in both cohorts to a maximum of 9.8% (average of ~2%) at day 9. In the presence of *B. infantis* and HMO, higher levels were maintained (average of ~2%) by day 14, whereas in the Abx-only cohort, levels had declined to <1% (Figure 3F). *Veillonella* is known to consume lactate, which is produced by *B. infantis* during HMO fermentation, so this may explain *Veillonella* enrichment. Abundant *Lactobacillus* may also increase lactate availability, and increased *Lactobacillus* during Abx dosing may explain early (day 9) increases in *Veillonella* in both cohorts. Additional changes in the *B. infantis* + HMO engrafted subset included significantly less Clostridiales at the end of the Abx dosing period (day 5) and less *Ruminococcus* at day 14 (Figure 3E; Wilcoxon's rank sum test, both $p_{adj} < 0.05$). Many of these changes were consistent in pairwise comparisons of all subjects in all three cohorts (Figures S2E–S2H, $p_{adj} < 0.05$; Figures S3A, S3C, S3E, S3G, S3I, and S3K). Significant increases in *Bifidobacterium* were noted at certain time points for all pairs of cohorts that were compared (Figures S2E–S2G). *Pediococcus* and *Lactobacillus* were also increased when the engrafted subset of the *B. infantis* + HMO cohort was compared with the *B. infantis*-only cohort (Figure S2H). With all subjects in the *B. infantis* + HMO cohort included, *Veillonella* was increased at day 14 compared with the Abx-only cohort (Figure S2E). Additionally, a repeated measures correlation of abundance of *Bifidobacterium* and *Veillonella* was significant for days 14 to 35 (Figure S3L; Spearman correlation r = 0.4227, p = 0.01).

Treatment with *B. infantis* and HMO during and after Abx disruption results in significant changes in gut metabolites

The impacts of *B. infantis* + HMO on fecal and serum metabolite profiles were explored using a fecal assay for SCFAs and lactate, an untargeted global fecal metabolomics method, and a targeted serum assay for microbiome-associated metabolites. To identify the most relevant changes associated with *B. infantis* engraftment, we focused on comparisons between engrafted subjects within the *B. infantis* + HMO cohort and the Abx-only control (Figure 4) but have also included comparisons between all subjects within the three cohorts (Figures S4 and S5).

As expected, Abx radically impacted microbially produced metabolite levels in both fecal and serum samples, with decreases from days 1 to 5 in, for example, SCFAs, secondary bile acids, and certain tryptophan and tyrosine metabolites (Figures 4, S4, and S5). Lactate increased in all subjects as well (Figures 4C and S4C), likely attributable to blooms of *Lactobacillaceae* (Figure 3).

Organic acids were expected to be at higher levels in engrafted subjects due to HMO fermentation by *B. infantis*.[65] However, analysis of SCFAs in stool samples may be confounded by differing absorption through the distal gastrointestinal tract.[41,66,67] Nonetheless, consistent with microbiome recovery after Abx dosing,[68,69] acetate levels increased in all cohorts after day 5 (Figures 4A and S4A). A significant difference between engrafted subjects in the *B. infantis* + HMO cohort and the Abx-only control was noted when acetate levels were analyzed over time (Figure 4A; mixed effects model, $p_{adj} = 0.03$). When all three cohorts were compared, with no emphasis on engraftment status, there was no significant difference (Figure S4A). Acetate in engrafted subjects in the *B. infantis* + HMO cohort recovered back to day 1 average levels and recovered significantly faster than in the Abx-only cohort, where two subjects were still not at baseline by day 35 (Figure 4B). An impact on recovery was also observed when all subjects in the *B. infantis* + HMO cohort were included (Figure S4B). *B. infantis* directly produces acetate and, indeed, increased acetate levels correlated with *B. infantis* abundance across days 5–28 in engrafted subjects in the *B. infantis* + HMO cohort (Table S5; Pearson $r^2 = 0.53$).

Lactate levels in stool were also significantly increased in the *B. infantis* + HMO cohort on days 11–28 compared with the Abx-only control (Figures 4C and S4C; mixed effects model, $p_{adj} = 0.03$). Consistent with an increase in organic acids, the pH of stool from subjects treated with *B. infantis* trended lower on all post-Abx days, with a significant difference at day 9 compared with the Abx-only control (Figure S4D; mixed effects model with Sidak's post test, $p_{adj} = 0.022$; 5.6 vs. 6.6). Although *B. infantis* production of acetate and lactate is thought to cross-feed SCFA producers and

Figure 3. Treatment with *B. infantis* and HMO results in microbiome changes following Abx perturbation
WMS analysis of stool samples.
(A) Shannon diversity of observed reads rarefied to 76,000 reads. Data are median and 95% confidence interval. Significance between time points and over time was determined for each of the three cohorts.
(B) Bray-Curtis dissimilarity for each sample with rarefied sequences aggregated to the genus level and displayed by cohort and day in a principal coordinate analysis (PCoA) plot specifically noting the trajectory from pre-treatment (day 1) to the end (day 5) of antibiotic dosing (arrow).
(C) Stacked bar charts displaying aggregated families at >1% abundance in each cohort on each day. Taxa <1% were assigned to "other." Where appropriate, subjects are separated into engrafted and not engrafted (NE).
(D) PCoA plots of Bray-Curtis dissimilarity calculated with rarefied sequences aggregated to the genus level for days 1, 5, and 14 only. The Abx-only control was compared with engrafted subjects in the *B. infantis* + HMO cohort, including (top row) and excluding (bottom row) taxa assigned to the genus *Bifidobacterium*.
(E) Volcano plot of aggregated genera >1% comparing abundance in the engrafted subjects in the *B. infantis* + HMO cohort vs. the Abx-only cohort. Log_2-fold change (centered log-ratio [CLR] transformed median value from 150 Dirichlet samples) and p values were plotted. Points with an adjusted p < 0.05 and >|0.6|-fold change are colored by taxon.
(F) Relative abundance of *Veillonella* over time in the Abx-only cohort (orange) and engrafted subjects receiving *B. infantis* + HMO (purple). Differences were calculated using CLR transformed abundances.
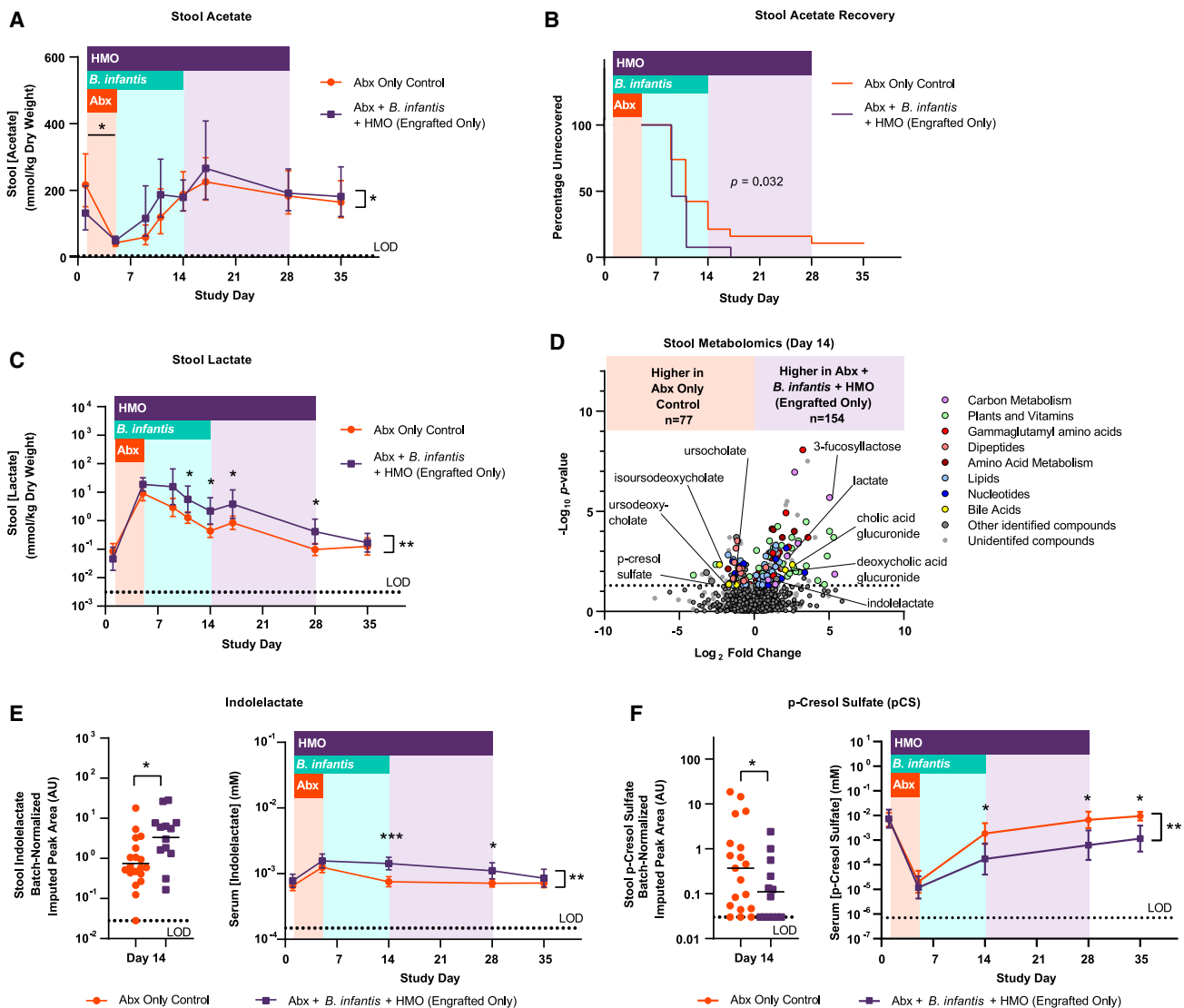See also Figures S2 and S3 and Table S4.

Figure 4. HMO-dependent engraftment with *B. infantis* following Abx perturbation results in changes in gut metabolites

(A and C) (A) Levels of acetic and (C) lactic acids in stool samples from subjects in the Abx-only cohort (n = 19) and engrafted subjects in the *B. infantis* + HMO cohort (n = 13). Data are geometric mean and 95% confidence intervals. Dotted lines represent LOD. Significance was determined between days 1 and 5 for individual cohorts in (A) and between cohorts at individual time points in (C).

(B) Kaplan-Meier curve plotting recovery of stool acetate back to baseline (the average of day 1 values across both cohorts).

(D) Volcano plot showing log$_2$ fold change in fecal metabolites on day 14 between engrafted subjects in the *B. infantis* + HMO cohort and the Abx-only cohort plotted against significance of the observed change. The dotted line represents p = 0.05. Metabolites that significantly differed are colored by category. Notable metabolites are labeled.

(E and F) Levels of (E) indolelactate and (F) p-cresol sulfate in stool at day 14 (left) and in serum at multiple time points (right). For scatterplot data, horizontal lines are geometric mean, and dotted lines are the imputed value for samples without detected signal. Time course data are geometric mean and 95% confidence interval, and dotted lines represent the limit of detection.

See also Figures S4 and S5 and Table S5.

promote the production of butyrate and propionate,[70] we found no difference in levels of butyrate or propionate in stool between cohorts over time (Figures S4E and S4F).

To look more broadly at the impact of *B. infantis* engraftment on the metabolome and the host, we employed two complementary approaches: global metabolomics analysis to compare the *B. infantis* + HMO and Abx-only cohorts at days 1, 5, and 14, and a quantitative targeted panel of microbial metabolites in

serum over time to highlight changes that reflect systemic impacts for all cohorts. As expected, fecal metabolite profiles were radically altered by Abx treatment (Figures S4G–S4P) but did not robustly differ between cohorts on day 1 or day 5, with the exception of detectable levels of HMOs in the cohort to which they were dosed (Figures S4I and S4M). On day 14, when *B. infantis* was at high levels in engrafted subjects, 231 metabolites significantly differed between engrafted subjects in the

B. infantis + HMO cohort compared with the Abx-only cohort (Figure 4D; Table S5; two-way repeated measures ANOVA, all $p_{adj} < 0.05$). A subset of these (56/231) were unidentified compounds, and others could be linked directly to treatment with *B. infantis* + HMO. For example, levels of 3-fucosyllactose (HMO) and the *B. infantis*-produced metabolites lactate and ILA were increased. When all subjects in the *B. infantis* + HMO cohort were included, 325 metabolites significantly differed between cohorts: 109 that gained significance and 15 that were no longer significantly different (Figure S4H; Table S5).

Similarly, metabolite levels in serum were robustly altered after Abx treatment (Figure S5A). When the engrafted subset of the *B. infantis* + HMO cohort and the Abx-only control were compared over time, eight metabolites differed: deoxycholate, pCS, ILA, phenyllactate, isovalerate, phenylacetic acid, 3-hydroxybenzoate, and phenylacetylglutamine (Table S5; mixed effects model with Sidak's post test, all $p_{adj} < 0.05$). ILA is a potentially beneficial immunomodulatory tryptophan metabolite, known to be produced by *B. infantis* and other gut microbes,[71–74] and was significantly elevated in engrafted subjects in both stool and serum at day 14 and in serum at day 28 (Figures 4E and S5B). This finding was maintained when all subjects from all three cohorts were included (Figures S5C–S5F).

The uremic toxin, pCS, was decreased in both stool and serum of subjects receiving *B. infantis* + HMO, regardless of engraftment status (Figures 4F, S5B, and S5G). pCS is a host-generated conjugate of p-cresol that contributes to inflammatory conditions and is produced from tyrosine or phenylalanine by intestinal bacteria.[75,76] Serum levels of other tyrosine and phenylalanine metabolites were also shifted, including decreases in the uremic toxins phenol sulfate and p-cresol-glucuronide (pCG) in engrafted subjects along with other intermediates (Figures S5B and S5H). Conversely, there were increases in serum 4-hydroxyphenylacetate, a precursor of p-cresol, and fecal and serum phenyllactate, from an alternative metabolic pathway present in *B. infantis* for tyrosine and phenylalanine (Figures S5B, S5C, S5H, and S5I; Table S5). Together, these changes suggest that high abundance of *B. infantis* supported by HMO may redirect tyrosine and phenylalanine flux away from production of inflammatory toxins.

Levels of several fecal bile acids differed between cohorts by global metabolomics analysis. Host-generated glucuronide conjugates of the primary bile acid cholate and its associated secondary bile acid deoxycholate were increased in the *B. infantis* + HMO cohort (Figures 4D and S4H). Additionally, the secondary bile acids ursocholate, ursodeoxycholate, and isoursodeoxycholate decreased (Figures 4D and S4H). Ursodeoxycholate was included in the serum analysis, but no changes were observed between cohorts for that or the bile acids chenodeoxycholate and cholate (Table S5). Interestingly, serum levels of the secondary bile acid deoxycholate significantly decreased in the *B. infantis* + HMO cohort over time (Table S5).

High-level engraftment of *B. infantis* influenced other fecal metabolites indicative of changes in microbial metabolism (Figure 4D). Over a quarter of the identified metabolites (47) were considered xenobiotics. Others were associated with carbohydrate metabolism (12), amino acids and derivatives (45), or lipid synthesis and metabolism (39), suggesting general shifts in microbial metabolism, gut mucosal properties, and/or enterocyte energetics. For example, increases in carbon sources, such as

sugar alcohols and plant-based molecules like feruloylquinates, suggested either decreased degradation or absorption of these molecules, and increases in eight gamma-glutamyl amino acids suggested altered protein degradation, similar to HMO-induced changes occurring in infants linked to lowered rates of respiratory illness.[77] When all subjects in the *B. infantis* + HMO cohort were included in the analysis, metabolites that gained significance included additional xenobiotics and core metabolic pathway intermediates.

Enhanced *in vitro* and *in vivo* growth of and production of propionate by *Veillonella* spp. co-cultured with *B. infantis* and HMO

Our data suggest that the introduction of *B. infantis* + HMO during and after Abx dosing enriches for *Veillonella*. *Veillonella* do not metabolize carbohydrates; rather, they consume lactate to produce propionate and acetate.[78] Thus, we hypothesized that expansion of this taxon was due to the elevated levels of lactate produced by *B. infantis* during growth on HMO (Figure 4C). To explore this potential cross-feeding relationship further, we isolated two *Veillonella* strains from stool of subjects in the *B. infantis* + HMO cohort and evaluated growth and SCFA production *in vitro* (Figures 5 and S6; Tukey's multiple comparisons of log-transformed data for all comparisons, p values detailed in Table S6). A commercially available strain of *Veillonella parvula* sourced from the human gut was used for comparison. Although growth kinetics varied, all *Veillonella* conformed to expectations by growing and producing propionate and acetate in a lactate-dependent manner (Figures 5A and S6A–S6E), while neither HMO alone nor *B. infantis* alone supported *Veillonella* growth or propionate production (Figures 5B–5D, S6F, and S6G). With both *B. infantis* and HMO, all *Veillonella* grew and produced propionate while consuming lactate (Figures 5B–5D, S6F, and S6G), supporting the model that cross-feeding led to increased abundance of *Veillonella* in the adult subjects in our study.

Increased *Veillonella* in subjects treated with *B. infantis* + HMO did not correspond to concomitant increases in fecal propionate (Figure S4F). Given that SCFAs like propionate may have been absorbed during transit, we employed a mouse model to sample across multiple gastrointestinal compartments. Germ-free mice were inoculated with *V. parvula* (or *B. infantis* as a control), stabilized for 1 week, and then given either PBS or *B. infantis* + HMO (Figure 6A). PBS or HMO treatment continued for 3 days. *V. parvula* levels increased over time in mice treated with *B. infantis* + HMO but not in the controls (Figure 6B; mixed effects model with Sidak's post test, $p_{adj} < 0.0001$). *B. infantis* was only detected when it was dosed (Figure S6I). After the final treatment, levels of propionate, lactate, and acetate in different intestinal segments were quantified (Figures 6C, 6D, and S6J). The cecum of mice colonized with *V. parvula* and subsequently treated with *B. infantis* + HMO had increased *Veillonella* abundance and propionate relative to PBS-treated mice (Figures 6C and S6H; mixed effects model, $p_{adj} = 0.0004$ and $p_{adj} = 0.0003$, respectively), indicating that cross-feeding occurred. In contrast, propionate did not significantly differ in rectal or fecal samples, reflecting previously observed variability in both rodents and humans.[41,67,79,80] Lactate levels were high in mice monocolonized with *B. infantis* and treated with HMO but lower in *V. parvula*-associated mice treated with *B. infantis* + HMO (Figure 6D), even though *B. infantis*
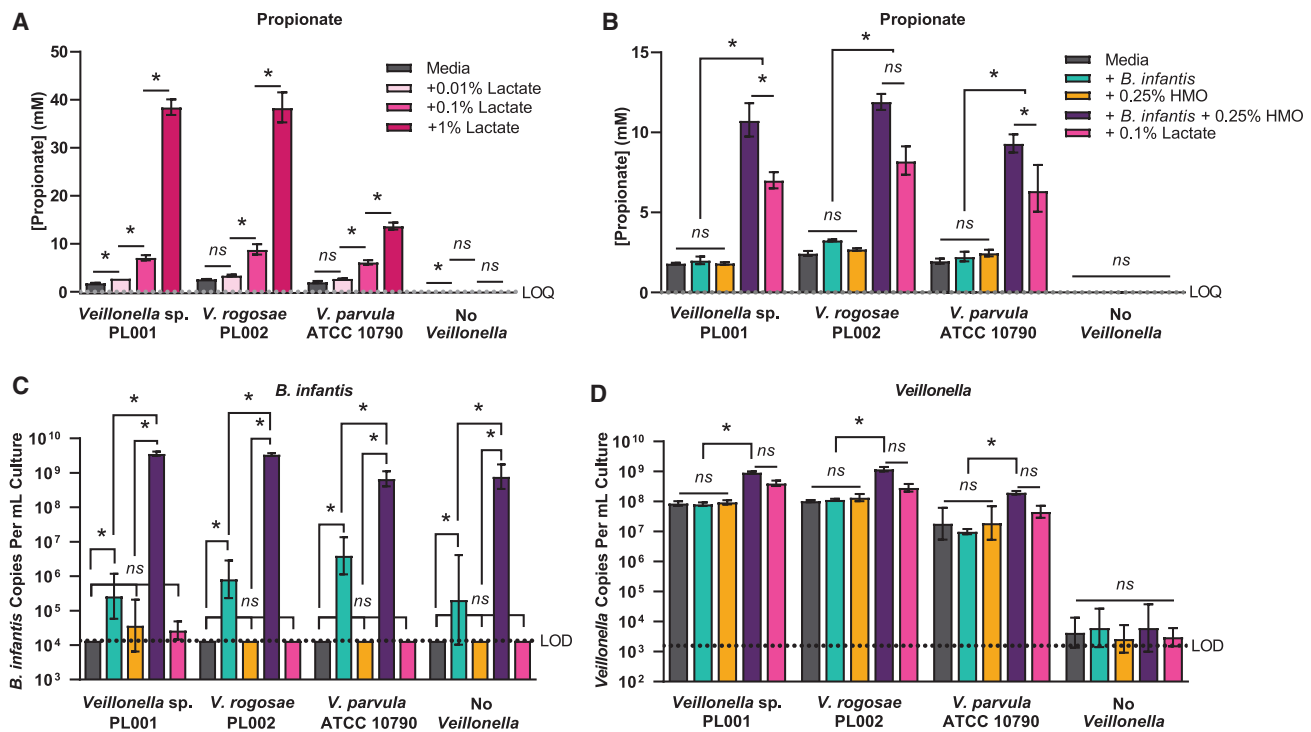
Cell Host & Microbe
Clinical and Translational Report

CellPress

Figure 5. *In vitro* cross-feeding of *Veillonella* species by *B. infantis* + HMO

(A) Propionate levels in *Veillonella* cultures after 30 h of growth in the indicated lactate concentrations. Propionate was measured using LC-MS/MS.

(B–D) Cultures were grown with or without *B. infantis*, HMO, or lactate. After 30 h, propionate (B), *B. infantis* (C), and *Veillonella* (D) were measured. Dotted lines indicate the limit of quantitation (A and B) or detection (C and D). Data represent the geometric mean and standard deviation of three independent experiments. *indicates $p_{adj} < 0.05$; "ns" indicates $p_{adj} > 0.05$; p values for all comparisons in Table S6.

See also Figure S6 and Table S6.

levels were similar for each group (Figure S6I), suggesting consumption of lactate by *Veillonella*.

Together, these *in vitro* and *in vivo* results are consistent with the observed increase in *Veillonella* in human trial subjects dosed with *B. infantis* + HMO, due to cross-feeding with the lactate produced by *B. infantis*. Further, these data suggest that local levels of propionate likely increased—at least transiently—in the gut of engrafted subjects, even though changes were not detected in stool or serum samples (Figures S4F and S5).

DISCUSSION

In this study, healthy adults were treated with Abx to induce a transient period of dysbiosis, allowing us to observe how HMO-dependent engraftment of *B. infantis* altered microbiome composition and function during recovery. We demonstrated high-level engraftment of *B. infantis* in ~76% of subjects receiving a synbiotic that consisted of *B. infantis* + HMO, with a maximum observed abundance of 81%. Accompanying changes in microbiome composition and gut metabolites reflected the influence of the synbiotic product on the gut environment.

In tandem with *B. infantis* engraftment, *Veillonella* was enriched in subjects receiving *B. infantis* + HMO, suggesting a cross-feeding relationship that is also supported by *in vitro* and mouse data. *Veillonella* are commensals in the human oral and gut microbiomes that consume lactate and produce the SCFAs propionate and acetate, which likely benefit the host.[63,78,81,82] One positive effect of propi-

onate is regulation of immune homeostasis by promoting the development of regulatory T cells.[83,84] Additionally, both propionate and acetate play a role in regulating glucose homeostasis and lipid metabolism and are linked to both satiety and improved control of glucose.[85] Propionate did not significantly increase in stool from our human subjects; however, it may have been rapidly utilized in the gut or subject to the variability reported for human fecal samples.[66] Indeed, our *in vivo* mouse data, where we observed increased propionate in cecal samples, but not rectal or fecal samples, point to differences between regions of the gastrointestinal tract.

We observed significant changes in host-active, microbially produced metabolites upon HMO-dependent engraftment of *B. infantis*. Increases were measured for ILA, a product of tryptophan metabolism by *B. infantis* and other bifidobacteria, both *in vitro* and in infants harboring *B. infantis*.[47,71,73,74] ILA was shown *in vitro* to have anti-inflammatory, immunomodulatory, and protective effects on immune and gut epithelial cells via activation of the aryl hydrocarbon receptor (AhR). Other indoles positively impact diseases including graft-vs.-host disease (GvHD),[86] colitis,[87–90] and gastrointestinal infection.[91] These activities are linked to the modulation of T cell differentiation and regulation of cytokines. Indoles are broadly known to bind AhR or the pregnane X receptor to influence the host.[92,93] However, binding affinities for AhR differ among indoles[94] and likely have distinct effects on downstream regulation,[95–97] so more investigation is needed to determine the specific impact of ILA.
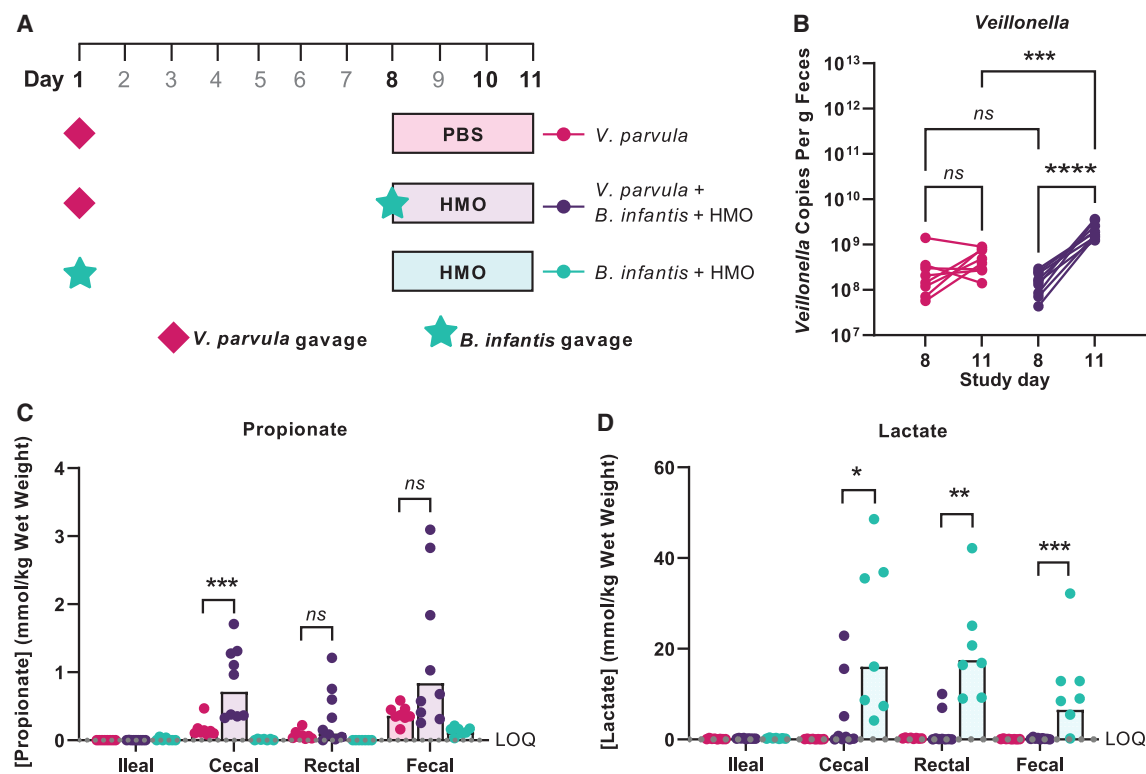
Figure 6. *In vivo* cross-feeding of *Veillonella* species by *B. infantis* + HMO

(A) A schematic of the study design. Germ-free mice were divided into three groups: two inoculated with *Veillonella parvula* and the third with *B. infantis* alone. After 1 week, the *V. parvula*-associated groups received either PBS or *B. infantis* + HMO; *B. infantis*-associated animals received HMO only. Over the subsequent 3 days, animals received once-daily gavages of PBS or HMO. Stool collection days are indicated in bold text.

(B) *Veillonella* levels were quantified in cage-bottom fecal pellets using qPCR. Each pair of connected symbols represents an individual mouse.

(C and D) Levels of propionate (C) and lactate (D) were measured in the contents of the indicated intestinal segments using LC-MS/MS. The dotted line indicates the limit of quantification (LOQ).

See also Figure S6.

HMO-dependent engraftment of *B. infantis* also resulted in changes indicative of altered flux through tyrosine metabolic pathways. For example, the microbially derived pro-inflammatory molecules pCS, pCG, and phenol sulfate were all decreased. Elevated levels of these molecules are associated with kidney disease,[98–100] gut barrier dysfunction,[101] and risk for GvHD.[102] Thus, a reduction of these uremic toxins may generally be beneficial.

In patient populations where administration of LBPs is linked to positive clinical outcomes, engraftment is thought to be necessary for efficacy.[5,6] Here, we show that our synbiotic not only leads to *B. infantis* engraftment but also drives a very high relative abundance. We propose that this is advantageous because it correlates with increased levels of certain beneficial microbial metabolites. In our study, lactate, acetate, and ILA, metabolites produced by *B. infantis*, all increased. These products cross-feed other organisms in the microbiome, triggering changes in downstream metabolites.

As expected, based on data from our previous human study,[24] *B. infantis* abundance and engraftment rate was higher when dosed in combination with HMO. HMO supplementation, especially at later time points, strongly enhanced the ability of *B. infantis* to influence microbiome community structure and gut metabolite levels.

The magnitude of the engraftment we achieved represents a >10,000-fold expansion of *B. infantis*. This compares favorably with reports of 10- to 100-fold expansion of LBPs upon engraftment in Abx-treated healthy adults[49] and reports of successful engraftment in dysbiotic patient populations, where presence/absence is used.[5,8,50] Our engraftment was comparable to levels observed in breastfed infants treated with a *B. infantis* probiotic.[46] The results presented here extend our previous findings in healthy adults and further predict that in patients suffering from profound and prolonged dysbiosis, *B. infantis* may reach equal or even greater levels than during the transient, Abx-induced dysbiosis observed in this study.

High levels of engrafted *B. infantis* corresponded with lower alpha diversity, which then rebounded after HMO dosing ended. Although diversity is typically considered a proxy measure for microbiome health, high-level engraftment of a single bacterial taxon may protect a low-diversity gut environment and allow for subsequent expansion of beneficial species. Indeed, HMO is theorized to have evolved in human milk to promote a high abundance of bifidobacteria in the infant gut.[27,30] In the infant gut, bifidobacteria are considered keystone species because they are primary degraders of glycans that cross-feed diverse bacterial taxa. Reduced bifidobacterial abundance affects

Cell Host & Microbe
Clinical and Translational Report

CellPress

development of the infant immune system, leading to, for example, inappropriate immune development and subsequent atopy and asthma.[103,104] High abundance may further protect against domination and subsequent infection by gastrointestinal pathogens.[105] Bifidobacteria may similarly benefit dysbiotic, fragile adult patient populations by, for example, preventing the domination by opportunistic pathogens that often precedes bloodstream infections in allogeneic hematopoietic stem cell transplant (allo-HCT) patients.[106–112] Microbial community composition and metabolites in this patient population have also been linked to risk of GvHD, an outcome resulting in high morbidity and mortality.[102,113] Altered levels of host-active metabolites during high-level *B. infantis* engraftment (for example, increases in SCFAs and ILA and decreases in pCS and phenol sulfate) may promote immune tolerance and thereby reduce GvHD.

In this study, we demonstrate that HMO-dependent *B. infantis* engraftment during transient dysbiosis leads to consistent changes in both microbiome composition and metabolic output. In certain patient populations, or during dysbioses induced by other classes of Abx, dysbiosis may not resolve without deliberate intervention. Our results represent a significant advance toward precision microbiome engineering to address such conditions, drawing from knowledge of the natural progression of healthy microbiome development in infants.

STAR★METHODS

Detailed methods are provided in the online version of this paper and include the following:

- KEY RESOURCES TABLE
- RESOURCE AVAILABILITY
  - Lead contact
  - Materials availability
  - Data and code availability
- EXPERIMENTAL MODEL AND SUBJECT DETAILS
  - Human subjects
  - Murine studies
  - Bacterial strains and growth conditions
- METHOD DETAILS
  - Healthy human subject study methods
  - Preparation of HMO Concentrate
  - Determination of pH of human stool
  - DNA extraction from human stool, quantification, and *B. infantis*-specific qPCR
  - Quantification of short-chain fatty acids and lactate in human stool
  - Quantification of metabolites in human serum
  - Global metabolomics analysis of human stool
  - Whole metagenomic sequencing and analyses
  - Determination of the susceptibility of *B. infantis* to vancomycin and metronidazole
  - Culturing and isolation of *Veillonella* strains
  - Assessment of growth and SCFA production of *Veillonella* strains during growth on lactate and co-culture with *B. infantis*
  - Murine model of *B. infantis* engraftment

- Quantification of short-chain fatty acids and lactate in mouse cecal contents and *in vitro* supernatants
- QUANTIFICATION AND STATISTICAL ANALYSIS

REFERENCES

1. Lawley, T.D., and Walker, A.W. (2013). Intestinal colonization resistance. Immunology *138*, 1–11. https://doi.org/10.1111/j.1365-2567.2012.03616.x.

2. Belkaid, Y., and Hand, T.W. (2014). Role of the microbiota in immunity and inflammation. Cell *157*, 121–141. https://doi.org/10.1016/j.cell.2014.03.011.

3. van Nood, E., Vrieze, A., Nieuwdorp, M., Fuentes, S., Zoetendal, E.G., de Vos, W.M., Visser, C.E., Kuijper, E.J., Bartelsman, J.F.W.M., Tijssen, J.G.P., et al. (2013). Duodenal infusion of donor feces for recurrent *Clostridium difficile*. N. Engl. J. Med. *368*, 407–415. https://doi.org/10.1056/NEJMoa1205037.

4. Feuerstadt, P., Louie, T.J., Lashner, B., Wang, E.E.L., Diao, L., Bryant, J.A., Sims, M., Kraft, C.S., Cohen, S.H., Berenson, C.S., et al. (2022). SER-109, an Oral microbiome therapy for recurrent *Clostridioides difficile* infection. N. Engl. J. Med. *386*, 220–229. https://doi.org/10.1056/NEJMoa2106516.

5. Aggarwala, V., Mogno, I., Li, Z., Yang, C., Britton, G.J., Chen-Liaw, A., Mitcham, J., Bongers, G., Gevers, D., Clemente, J.C., et al. (2021). Precise quantification of bacterial strains after fecal microbiota transplantation delineates long-term engraftment and explains outcomes. Nat. Microbiol. *6*, 1309–1318. https://doi.org/10.1038/s41564-021-00966-0.

6. Ianiro, G., Punčochář, M., Karcher, N., Porcari, S., Armanini, F., Asnicar, F., Beghini, F., Blanco-Míguez, A., Cumbo, F., Manghi, P., et al. (2022).

Variability of strain engraftment and predictability of microbiome composition after fecal microbiota transplantation across different diseases. Nat. Med. 28, 1913–1923. https://doi.org/10.1038/s41591-022-01964-3.

7. Danne, C., Rolhion, N., and Sokol, H. (2021). Recipient factors in faecal microbiota transplantation: one stool does not fit all. Nat. Rev. Gastroenterol. Hepatol. 18, 503–513. https://doi.org/10.1038/s41575-021-00441-5.

8. Li, S.S., Zhu, A., Benes, V., Costea, P.I., Hercog, R., Hildebrand, F., Huerta-Cepas, J., Nieuwdorp, M., Salojärvi, J., Voigt, A.Y., et al. (2016). Durable coexistence of donor and recipient strains after fecal microbiota transplantation. Science 352, 586–589. https://doi.org/10.1126/science.aad8852.

9. Maldonado-Gómez, M.X., Martínez, I., Bottacini, F., O'Callaghan, A., Ventura, M., van Sinderen, D., Hillmann, B., Vangay, P., Knights, D., Hutkins, R.W., et al. (2016). Stable engraftment of Bifidobacterium longum AH1206 in the human gut depends on individualized features of the resident microbiome. Cell Host Microbe 20, 515–526. https://doi.org/10.1016/j.chom.2016.09.001.

10. Smillie, C.S., Sauk, J., Gevers, D., Friedman, J., Sung, J., Youngster, I., Hohmann, E.L., Staley, C., Khoruts, A., Sadowsky, M.J., et al. (2018). Strain tracking reveals the determinants of bacterial engraftment in the human gut following fecal microbiota transplantation. Cell Host Microbe 23, 229–240.e5. https://doi.org/10.1016/j.chom.2018.01.003.

11. Sorbara, M.T., and Pamer, E.G. (2022). Microbiome-based therapeutics. Nat. Rev. Microbiol. 20, 365–380. https://doi.org/10.1038/s41579-021-00667-9.

12. Ducarmon, Q.R., Kuijper, E.J., and Olle, B. (2021). Opportunities and challenges in development of live biotherapeutic products to fight infections. J. Infect. Dis. 223, S283–S289. https://doi.org/10.1093/infdis/jiaa779.

13. Alander, M., Mättö, J., Kneifel, W., Johansson, M., Kögler, B., Crittenden, R., Mattila-Sandholm, T., and Saarela, M. (2001). Effect of galacto-oligosaccharide supplementation on human faecal microflora and on survival and persistence of Bifidobacterium lactis Bb-12 in the gastrointestinal tract. Int. Dairy J. 11, 817–825. https://doi.org/10.1016/S0958-6946(01)00100-5.

14. Charbonneau, D., Gibb, R.D., and Quigley, E.M.M. (2013). Fecal excretion of Bifidobacterium infantis 35624 and changes in fecal microbiota after eight weeks of oral supplementation with encapsulated probiotic. Gut Microbes 4, 201–211. https://doi.org/10.4161/gmic.24196.

15. Firmesse, O., Mogenet, A., Bresson, J.-L., Corthier, G., and Furet, J.-P. (2008). Lactobacillus rhamnosus R11 consumed in a food supplement survived human digestive transit without modifying microbiota equilibrium as assessed by real-time polymerase chain reaction. J. Mol. Microbiol. Biotechnol. 14, 90–99. https://doi.org/10.1159/000106087.

16. Frese, S.A., Hutkins, R.W., and Walter, J. (2012). Comparison of the colonization ability of autochthonous and allochthonous strains of lactobacilli in the human gastrointestinal tract. Adv. Microbiol. 02, 399–409. https://doi.org/10.4236/aim.2012.23051.

17. Malinen, E., Mättö, J., Salmitie, M., Alander, M., Saarela, M., and Palva, A. (2002). PCR-ELISAII: analysis of Bifidobacterium populations in human faecal samples from a consumption trial with Bifidobacterium lactis Bb-12 and a galacto-oligosaccharide preparation. Syst. Appl. Microbiol. 25, 249–258. https://doi.org/10.1078/0723-2020-00117.

18. Rattanaprasert, M., Roos, S., Hutkins, R.W., and Walter, J. (2014). Quantitative evaluation of synbiotic strategies to improve persistence and metabolic activity of Lactobacillus reuteri DSM 17938 in the human gastrointestinal tract. J. Funct. Foods 10, 85–94. https://doi.org/10.1016/j.jff.2014.05.017.

19. Rochet, V., Rigottier-Gois, L., Levenez, F., Cadiou, J., Marteau, P., Bresson, J.-L., Goupil-Feuillerat, N., and Doré, J. (2008). Modulation of Lactobacillus casei in ileal and fecal samples from healthy volunteers after consumption of a fermented milk containing Lactobacillus casei DN-114 001 [Rif]. Can. J. Microbiol. 54, 660–667. https://doi.org/10.1139/W08-050.

20. Zmora, N., Zilberman-Schapira, G., Suez, J., Mor, U., Dori-Bachash, M., Bashiardes, S., Kotler, E., Zur, M., Regev-Lehavi, D., Brik, R.B.-Z., et al. (2018). Personalized gut mucosal colonization resistance to empiric probiotics is associated with unique Host and Microbiome Features. Cell 174, 1388–1405.e21. https://doi.org/10.1016/j.cell.2018.08.041.

21. Shepherd, E.S., DeLoache, W.C., Pruss, K.M., Whitaker, W.R., and Sonnenburg, J.L. (2018). An exclusive metabolic niche enables strain engraftment in the gut microbiota. Nature 557, 434–438. https://doi.org/10.1038/s41586-018-0092-4.

22. Kearney, S.M., Gibbons, S.M., Erdman, S.E., and Alm, E.J. (2018). Orthogonal dietary niche enables reversible engraftment of a gut bacterial commensal. Cell Rep. 24, 1842–1851. https://doi.org/10.1016/j.celrep.2018.07.032.

23. Heiss, B.E., Ehrlich, A.M., Maldonado-Gomez, M.X., Taft, D.H., Larke, J.A., Goodson, M.L., Slupsky, C.M., Tancredi, D.J., Raybould, H.E., and Mills, D.A. (2021). Bifidobacterium catabolism of human milk oligosaccharides overrides endogenous competitive exclusion driving colonization and protection. Gut Microbes 13, 1986666. https://doi.org/10.1080/19490976.2021.1986666.

24. Button, J.E., Autran, C.A., Reens, A.L., Cosetta, C.M., Smriga, S., Ericson, M., Pierce, J.V., Cook, D.N., Lee, M.L., Sun, A.K., et al. (2022). Dosing a synbiotic of human milk oligosaccharides and B. infantis leads to reversible engraftment in healthy adult microbiomes without antibiotics. Cell Host Microbe 30, 712–725.e7. https://doi.org/10.1016/j.chom.2022.04.001.

25. German, J.B., Freeman, S.L., Lebrilla, C.B., and Mills, D.A. (2008). Human milk oligosaccharides: evolution, structures and bioselectivity as substrates for intestinal bacteria. discussion 218–222. Nestle Nutr. Workshop Ser. Pediatr. Program. 62, 205–218. https://doi.org/10.1159/000146322.

26. Bode, L. (2012). Human milk oligosaccharides: every baby needs a sugar mama. Glycobiology 22, 1147–1162. https://doi.org/10.1093/glycob/cws074.

27. Marcobal, A., and Sonnenburg, J.L. (2012). Human milk oligosaccharide consumption by intestinal microbiota. Clin. Microbiol. Infect. 18, 12–15. https://doi.org/10.1111/j.1469-0691.2012.03863.x.

28. Newburg, D.S., and Morelli, L. (2015). Human milk and infant intestinal mucosal glycans guide succession of the neonatal intestinal microbiota. Pediatr. Res. 77, 115–120. https://doi.org/10.1038/pr.2014.178.

29. Medina, D.A., Pinto, F., Ovalle, A., Thomson, P., and Garrido, D. (2017). Prebiotics mediate microbial interactions in a consortium of the infant gut microbiome. Int. J. Mol. Sci. 18, 2095. https://doi.org/10.3390/ijms18102095.

30. Underwood, M.A., German, J.B., Lebrilla, C.B., and Mills, D.A. (2015). Bifidobacterium longum subspecies infantis: champion colonizer of the infant gut. Pediatr. Res. 77, 229–235. https://doi.org/10.1038/pr.2014.156.

31. Sela, D.A., Chapman, J., Adeuya, A., Kim, J.H., Chen, F., Whitehead, T.R., Lapidus, A., Rokhsar, D.S., Lebrilla, C.B., German, J.B., et al. (2008). The genome sequence of Bifidobacterium longum subsp. infantis reveals adaptations for milk utilization within the infant microbiome. Proc. Natl. Acad. Sci. USA 105, 18964–18969. https://doi.org/10.1073/pnas.0809584105.

32. LoCascio, R.G., Desai, P., Sela, D.A., Weimer, B., and Mills, D.A. (2010). Broad conservation of milk utilization genes in Bifidobacterium longum subsp. infantis as revealed by comparative genomic hybridization. Appl. Environ. Microbiol. 76, 7373–7381. https://doi.org/10.1128/AEM.00675-10.

33. Gotoh, A., Katoh, T., Sakanaka, M., Ling, Y., Yamada, C., Asakuma, S., Urashima, T., Tomabechi, Y., Katayama-Ikegami, A., Kurihara, S., et al. (2018). Sharing of human milk oligosaccharides degradants within bifidobacterial communities in faecal cultures supplemented with Bifidobacterium bifidum. Sci. Rep. 8, 13958. https://doi.org/10.1038/s41598-018-32080-3.

34. Belenguer, A., Duncan, S.H., Calder, A.G., Holtrop, G., Louis, P., Lobley, G.E., and Flint, H.J. (2006). Two routes of metabolic cross-feeding between Bifidobacterium adolescentis and butyrate-producing anaerobes from the human gut. Appl. Environ. Microbiol. 72, 3593–3599. https://doi.org/10.1128/AEM.72.5.3593-3599.2006.

35. Chia, L.W., Mank, M., Blijenberg, B., Bongers, R.S., van Limpt, K., Wopereis, H., Tims, S., Stahl, B., Belzer, C., and Knol, J. (2021).

Cell Host & Microbe
Clinical and Translational Report

Cross-feeding between *Bifidobacterium infantis* and *Anaerostipes caccae* on lactose and human milk oligosaccharides. Benef. Microbes *12*, 69–83. https://doi.org/10.3920/BM2020.0005.

36. Duncan, S.H., Louis, P., and Flint, H.J. (2004). Lactate-utilizing bacteria, isolated from human feces, that produce butyrate as a major fermentation product. Appl. Environ. Microbiol. *70*, 5810–5817. https://doi.org/10.1128/AEM.70.10.5810-5817.2004.

37. Duncan, S.H., Holtrop, G., Lobley, G.E., Calder, A.G., Stewart, C.S., and Flint, H.J. (2004). Contribution of acetate to butyrate formation by human faecal bacteria. Br. J. Nutr. *91*, 915–923. https://doi.org/10.1079/BJN20041150.

38. Falony, G., Vlachou, A., Verbrugghe, K., and De Vuyst, L.D. (2006). Cross-feeding between *Bifidobacterium longum* BB536 and acetate-converting, butyrate-producing colon bacteria during growth on oligofructose. Appl. Environ. Microbiol. *72*, 7835–7841. https://doi.org/10.1128/AEM.01296-06.

39. Rivière, A., Gagnon, M., Weckx, S., Roy, D., and De Vuyst, L.D. (2015). Mutual cross-feeding interactions between *Bifidobacterium longum* subsp. *longum* NCC2705 and *Eubacterium rectale* ATCC 33656 explain the bifidogenic and butyrogenic effects of arabinoxylan oligosaccharides. Appl. Environ. Microbiol. *81*, 7767–7781. https://doi.org/10.1128/AEM.02089-15.

40. Schwab, C., Ruscheweyh, H.-J., Bunesova, V., Pham, V.T., Beerenwinkel, N., and Lacroix, C. (2017). Trophic interactions of infant bifidobacteria and *Eubacterium hallii* during L-fucose and fucosyllactose degradation. Front. Microbiol. *8*, 95. https://doi.org/10.3389/fmicb.2017.00095.

41. Cummings, J.H., Pomare, E.W., Branch, W.J., Naylor, C.P., and Macfarlane, G.T. (1987). Short chain fatty acids in human large intestine, portal, hepatic and venous blood. Gut *28*, 1221–1227. https://doi.org/10.1136/gut.28.10.1221.

42. Koh, A., De Vadder, F.D., Kovatcheva-Datchary, P., and Bäckhed, F. (2016). From dietary fiber to host physiology: short-chain fatty acids as key bacterial metabolites. Cell *165*, 1332–1345. https://doi.org/10.1016/j.cell.2016.05.041.

43. Bergmann, K.R., Liu, S.X.L., Tian, R., Kushnir, A., Turner, J.R., Li, H.-L., Chou, P.M., Weber, C.R., and De Plaen, I.G. (2013). Bifidobacteria stabilize claudins at tight junctions and prevent intestinal barrier dysfunction in mouse necrotizing enterocolitis. Am. J. Pathol. *182*, 1595–1606. https://doi.org/10.1016/j.ajpath.2013.01.013.

44. Ríos-Covián, D., Ruas-Madiedo, P., Margolles, A., Gueimonde, M., de los Reyes-Gavilán, C.G., and Salazar, N. (2016). Intestinal short chain fatty acids and their link with diet and human health. Front. Microbiol. *7*, 185. https://doi.org/10.3389/fmicb.2016.00185.

45. Underwood, M.A., Arriola, J., Gerber, C.W., Kaveti, A., Kalanetra, K.M., Kananurak, A., Bevins, C.L., Mills, D.A., and Dvorak, B. (2014). *Bifidobacterium longum* subsp. *infantis* in experimental necrotizing enterocolitis: alterations in inflammation, innate immune response and the microbiota. Pediatr. Res. *76*, 326–333. https://doi.org/10.1038/pr.2014.102.

46. Frese, S.A., Hutton, A.A., Contreras, L.N., Shaw, C.A., Palumbo, M.C., Casaburi, G., Xu, G., Davis, J.C.C., Lebrilla, C.B., Henrick, B.M., et al. (2017). Persistence of supplemented *Bifidobacterium longum* subsp. *infantis* EVC001 in breastfed infants. mSphere *2*, e00501–e00517. https://doi.org/10.1128/mSphere.00501-17.

47. Henrick, B.M., Rodriguez, L., Lakshmikanth, T., Pou, C., Henckel, E., Arzoomand, A., Olin, A., Wang, J., Mikes, J., Tan, Z., et al. (2021). Bifidobacteria-mediated immune system imprinting early in life. Cell *184*, 3884–3898.e11. https://doi.org/10.1016/j.cell.2021.05.030.

48. Casaburi, G., and Frese, S.A. (2018). Colonization of breastfed infants by *Bifidobacterium longum* subsp. *infantis* EVC001 reduces virulence gene abundance. Hum. Microbiome J. *9*, 7–10. https://doi.org/10.1016/j.humic.2018.05.001.

49. Bobilev, D., Bhattarai, S., Menon, R., Klein, B., Reddy, S., Olle, B., Roberts, B., Bucci, V., and Norman, J. (2019). 1953. VE303, a rationally designed bacterial consortium for prevention of recurrent *Clostridioides difficile* (*C. difficile*) infection (rCDI), stably restores the gut microbiota after vancomycin (vanco)-Induced dysbiosis in adult healthy volunteers (HV). Open Forum Infect. Dis. *6*, S60. https://doi.org/10.1093/ofid/ofz359.130.

50. McGovern, B.H., Ford, C.B., Henn, M.R., Pardi, D.S., Khanna, S., Hohmann, E.L., O'Brien, E.J., Desjardins, C.A., Bernardo, P., Wortman, J.R., et al. (2021). SER-109, an investigational microbiome drug to reduce recurrence after *Clostridioides difficile* infection: lessons learned from a Phase 2 trial. Clin. Infect. Dis. *72*, 2132–2140. https://doi.org/10.1093/cid/ciaa387.

51. Dethlefsen, L., and Relman, D.A. (2011). Incomplete recovery and individualized responses of the human distal gut microbiota to repeated antibiotic perturbation. Proc. Natl. Acad. Sci. USA *108*, 4554–4561. https://doi.org/10.1073/pnas.1000087107.

52. Rashid, M.-U., Zaura, E., Buijs, M.J., Keijser, B.J.F., Crielaard, W., Nord, C.E., and Weintraub, A. (2015). Determining the long-term effect of antibiotic administration on the human normal intestinal microbiota using culture and Pyrosequencing methods. Clin. Infect. Dis. *60*, S77–S84. https://doi.org/10.1093/cid/civ137.

53. Zaura, E., Brandt, B.W., Teixeira de Mattos, M.J., Buijs, M.J., Caspers, M.P.M., Rashid, M.-U., Weintraub, A., Nord, C.E., Savell, A., Hu, Y., et al. (2015). Same Exposure but Two Radically Different Responses to antibiotics: resilience of the Salivary microbiome versus Long-Term Microbial Shifts in Feces. mBio *6*, e01693-e01615. https://doi.org/10.1128/mBio.01693-15.

54. Palleja, A., Mikkelsen, K.H., Forslund, S.K., Kashani, A., Allin, K.H., Nielsen, T., Hansen, T.H., Liang, S., Feng, Q., Zhang, C., et al. (2018). Recovery of gut microbiota of healthy adults following antibiotic exposure. Nat. Microbiol. *3*, 1255–1265. https://doi.org/10.1038/s41564-018-0257-9.

55. Suez, J., Zmora, N., Zilberman-Schapira, G., Mor, U., Dori-Bachash, M., Bashiardes, S., Zur, M., Regev-Lehavi, D., Ben-Zeev Brik, R., Federici, S., et al. (2018). Post-antibiotic gut mucosal microbiome reconstitution is impaired by probiotics and improved by autologous FMT. Cell *174*, 1406–1423.e16. https://doi.org/10.1016/j.cell.2018.08.047.

56. Schwartz, D.J., Langdon, A.E., and Dantas, G. (2020). Understanding the impact of antibiotic perturbation on the human microbiome. Genome Med. *12*, 82. https://doi.org/10.1186/s13073-020-00782-x.

57. Chang, J.Y., Antonopoulos, D.A., Kalra, A., Tonelli, A., Khalife, W.T., Schmidt, T.M., and Young, V.B. (2008). Decreased diversity of the fecal microbiome in recurrent *Clostridium difficile* –Associated diarrhea. J. Infect. Dis. *197*, 435–438. https://doi.org/10.1086/525047.

58. Montassier, E., Gastinne, T., Vangay, P., Al-Ghalith, G.A., Bruley des Varannes, S., Massart, S., Moreau, P., Potel, G., de La Cochetière, M.F., Batard, E., et al. (2015). Chemotherapy-driven dysbiosis in the intestinal microbiome. Aliment. Pharmacol. Ther. *42*, 515–528. https://doi.org/10.1111/apt.13302.

59. Sonnenburg, E.D., Smits, S.A., Tikhonov, M., Higginbottom, S.K., Wingreen, N.S., and Sonnenburg, J.L. (2016). Diet-induced extinctions in the gut microbiota compound over generations. Nature *529*, 212–215. https://doi.org/10.1038/nature16504.

60. Arthur, J.C., Perez-Chanona, E., Mühlbauer, M., Tomkovich, S., Uronis, J.M., Fan, T.-J., Campbell, B.J., Abujamel, T., Dogan, B., Rogers, A.B., et al. (2012). Intestinal inflammation targets cancer-inducing activity of the microbiota. Science *338*, 120–123. https://doi.org/10.1126/science.1224820.

61. Isaac, S., Scher, J.U., Djukovic, A., Jiménez, N., Littman, D.R., Abramson, S.B., Pamer, E.G., and Ubeda, C. (2017). Short- and long-term effects of oral vancomycin on the human intestinal microbiota. J. Antimicrob. Chemother. *72*, 128–136. https://doi.org/10.1093/jac/dkw383.

62. Pilla, R., Gaschen, F.P., Barr, J.W., Olson, E., Honneffer, J., Guard, B.C., Blake, A.B., Villanueva, D., Khattab, M.R., AlShawaqfeh, M.K., et al. (2020). Effects of metronidazole on the fecal microbiome and metabolome in healthy dogs. J. Vet. Intern. Med. *34*, 1853–1866. https://doi.org/10.1111/jvim.15871.

63. Lloyd-Price, J., Mahurkar, A., Rahnavard, G., Crabtree, J., Orvis, J., Hall, A.B., Brady, A., Creasy, H.H., McCracken, C., Giglio, M.G., et al. (2017). Strains, functions and dynamics in the expanded Human Microbiome Project. Nature 550, 61–66. https://doi.org/10.1038/nature23889.

64. Amir, A., McDonald, D., Navas-Molina, J.A., Debelius, J., Morton, J.T., Hyde, E., Robbins-Pianka, A., and Knight, R. (2017). Correcting for microbial blooms in fecal samples during room-temperature shipping. mSystems 2. e00199-e00116. https://doi.org/10.1128/mSystems.00199-16.

65. Pokusaeva, K., Fitzgerald, G.F., and van Sinderen, D. (2011). Carbohydrate metabolism in bifidobacteria. Genes Nutr. 6, 285–306. https://doi.org/10.1007/s12263-010-0206-6.

66. McOrist, A.L., Abell, G.C.J., Cooke, C., and Nyland, K. (2008). Bacterial population dynamics and faecal short-chain fatty acid (SCFA) concentrations in healthy humans. Br. J. Nutr. 100, 138–146. https://doi.org/10.1017/S0007114507886351.

67. Genda, T., Kondo, T., Sugiura, S., Hino, S., Shimamoto, S., Nakamura, T., Ukita, S., and Morita, T. (2018). Bacterial fermentation of water-soluble cellulose acetate raises large-bowel acetate and propionate and decreases plasma cholesterol concentrations in rats. J. Agric. Food Chem. 66, 11909–11916. https://doi.org/10.1021/acs.jafc.8b04093.

68. Høverstad, T., Carlstedt-Duke, B., Lingaas, E., Norin, E., Saxerholt, H., Steinbakk, M., and Midtvedt, T. (1986). Influence of oral intake of seven different antibiotics on faecal short-chain fatty acid excretion in healthy subjects. Scand. J. Gastroenterol. 21, 997–1003. https://doi.org/10.3109/00365528608996411.

69. Høverstad, T., Carlstedt-Duke, B., Lingaas, E., Midtvedt, T., Norin, K.E., Saxerholt, H., and Steinbakk, M. (1986). Influence of ampicillin, clindamycin, and metronidazole on faecal excretion of short-chain fatty acids in healthy subjects. Scand. J. Gastroenterol. 21, 621–626. https://doi.org/10.3109/00365528609003109.

70. Milani, C., Duranti, S., Bottacini, F., Casey, E., Turroni, F., Mahony, J., Belzer, C., Delgado Palacio, S., Arboleya Montes, S., Mancabelli, L., et al. (2017). The first microbial colonizers of the human gut: composition, activities, and health implications of the infant gut microbiota. Microbiol. Mol. Biol. Rev. 81. e00036-e00017. https://doi.org/10.1128/MMBR.00036-17.

71. Laursen, M.F., Sakanaka, M., von Burg, N., Mörbe, U., Andersen, D., Moll, J.M., Pekmez, C.T., Rivollier, A., Michaelsen, K.F., Mølgaard, C., et al. (2021). Bifidobacterium species associated with breastfeeding produce aromatic lactic acids in the infant gut. Nat. Microbiol. 6, 1367–1382. https://doi.org/10.1038/s41564-021-00970-4.

72. Sakurai, T., Odamaki, T., and Xiao, J.Z. (2019). Production of indole-3-lactic acid by Bifidobacterium Strains isolated from human infants. Microorganisms 7, 340. https://doi.org/10.3390/microorganisms7090340.

73. Ehrlich, A.M., Pacheco, A.R., Henrick, B.M., Taft, D., Xu, G., Huda, M.N., Mishchuk, D., Goodson, M.L., Slupsky, C., Barile, D., et al. (2020). Indole-3-lactic acid associated with Bifidobacterium-dominated microbiota significantly decreases inflammation in intestinal epithelial cells. BMC Microbiol. 20, 357. https://doi.org/10.1186/s12866-020-02023-y.

74. Meng, D., Sommella, E., Salviati, E., Campiglia, P., Ganguli, K., Djebali, K., Zhu, W., and Walker, W.A. (2020). Indole-3-lactic acid, a metabolite of tryptophan, secreted by Bifidobacterium longum subspecies infantis is anti-inflammatory in the immature intestine. Pediatr. Res. 88, 209–217. https://doi.org/10.1038/s41390-019-0740-x.

75. Saito, Y., Sato, T., Nomoto, K., and Tsuji, H. (2018). Identification of phenol- and p-cresol-producing intestinal bacteria by using media supplemented with tyrosine and its metabolites. FEMS Microbiol. Ecol. 94, fiy125. https://doi.org/10.1093/femsec/fiy125.

76. Gryp, T., De Paepe, K., Vanholder, R., Kerckhof, F.-M., Van Biesen, W., Van de Wiele, T., Verbeke, F., Speeckaert, M., Joossens, M., Couttenye, M.M., et al. (2020). Gut microbiota generation of protein-bound uremic toxins and related metabolites is not altered at different stages of chronic kidney disease. Kidney Int. 97, 1230–1242. https://doi.org/10.1016/j.kint.2020.01.028.

77. Martin, F.-P., Tytgat, H.L.P., Krogh Pedersen, H., Moine, D., Eklund, A.C., Berger, B., and Sprenger, N. (2022). Host-microbial co-metabolites modulated by human milk oligosaccharides relate to reduced risk of respiratory tract infections. Front. Nutr. 9, 935711. https://doi.org/10.3389/fnut.2022.935711.

78. Ng, S.K.C., and Hamilton, I.R. (1971). Lactate metabolism by Veillonella parvula. J. Bacteriol. 105, 999–1005. https://doi.org/10.1128/jb.105.3.999-1005.1971.

79. Zhen, Y., Ge, L., Xu, Q., Hu, L., Wei, W., Huang, J., Loor, J.J., Yang, Q., Wang, M., and Zhou, P. (2022). Normal Light-Dark and short-light cycles regulate intestinal inflammation, circulating short-chain fatty acids and gut microbiota in Period2 gene knockout mice. Front. Immunol. 13, 848248. https://doi.org/10.3389/fimmu.2022.848248.

80. Chen, D., Yu, J., Zhang, Z., Su, X., Li, L., and Li, L. (2019). Controlling pre-analytical process in high-coverage quantitative metabolomics: spot-sample collection for mouse urine and fecal metabolome profiling. Anal. Chem. 91, 4958–4963. https://doi.org/10.1021/acs.analchem.9b00310.

81. Ng, S.K.C., and Hamilton, I.R. (1973). Carbon dioxide fixation by Veillonella parvula M$_4$ and its relation to propionic acid formation. Can. J. Microbiol. 19, 715–723. https://doi.org/10.1139/m73-116.

82. Asnicar, F., Berry, S.E., Valdes, A.M., Nguyen, L.H., Piccinno, G., Drew, D.A., Leeming, E., Gibson, R., Le Roy, C., Khatib, H.A., et al. (2021). Microbiome connections with host metabolism and habitual diet from 1,098 deeply phenotyped individuals. Nat. Med. 27, 321–332. https://doi.org/10.1038/s41591-020-01183-8.

83. Smith, P.M., Howitt, M.R., Panikov, N., Michaud, M., Gallini, C.A., Bohlooly-Y, M., Glickman, J.N., and Garrett, W.S. (2013). The Microbial Metabolites, Short-Chain Fatty Acids, Regulate Colonic T$_{reg}$ Cell Homeostasis. Science 341, 569–573. https://doi.org/10.1126/science.1241165.

84. Arpaia, N., Campbell, C., Fan, X., Dikiy, S., van der Veeken, J., deRoos, P., Liu, H., Cross, J.R., Pfeffer, K., Coffer, P.J., et al. (2013). Metabolites produced by commensal bacteria promote peripheral regulatory T-cell generation. Nature 504, 451–455. https://doi.org/10.1038/nature12726.

85. Morrison, D.J., and Preston, T. (2016). Formation of short chain fatty acids by the gut microbiota and their impact on human metabolism. Gut Microbes 7, 189–200. https://doi.org/10.1080/19490976.2015.1134082.

86. Swimm, A., Giver, C.R., DeFilipp, Z., Rangaraju, S., Sharma, A., Ulezko Antonova, A., Sonowal, R., Capaldo, C., Powell, D., Qayed, M., et al. (2018). Indoles derived from intestinal microbiota act via type I interferon signaling to limit graft-versus-host disease. Blood 132, 2506–2519. https://doi.org/10.1182/blood-2018-03-838193.

87. Flannigan, K.L., Nieves, K.M., Szczepanski, H.E., Serra, A., Lee, J.W., Alston, L.A., Ramay, H., Mani, S., and Hirota, S.A. (2023). The pregnane X receptor and indole-3-propionic acid shape the intestinal mesenchyme to restrain inflammation and fibrosis. Cell. Mol. Gastroenterol. Hepatol. 15, 765–795. https://doi.org/10.1016/j.jcmgh.2022.10.014.

88. Aoki, R., Aoki-Yoshida, A., Suzuki, C., and Takayama, Y. (2018). Indole-3-pyruvic acid, an aryl hydrocarbon receptor activator, suppresses experimental colitis in mice. J. Immunol. 201, 3683–3693. https://doi.org/10.4049/jimmunol.1701734.

89. Alexeev, E.E., Lanis, J.M., Kao, D.J., Campbell, E.L., Kelly, C.J., Battista, K.D., Gerich, M.E., Jenkins, B.R., Walk, S.T., Kominsky, D.J., et al. (2018). Microbiota-derived indole metabolites promote human and murine intestinal homeostasis through regulation of interleukin-10 receptor. Am. J. Pathol. 188, 1183–1194. https://doi.org/10.1016/j.ajpath.2018.01.011.

90. Peng, C., Wu, C., Xu, X., Pan, L., Lou, Z., Zhao, Y., Jiang, H., He, Z., and Ruan, B. (2021). Indole-3-carbinol ameliorates necroptosis and inflammation of intestinal epithelial cells in mice with ulcerative colitis by activating aryl hydrocarbon receptor. Exp. Cell Res. 404, 112638. https://doi.org/10.1016/j.yexcr.2021.112638.

91. Zelante, T., Iannitti, R.G., Cunha, C., De Luca, A., Giovannini, G., Pieraccini, G., Zecchi, R., D'Angelo, C., Massi-Benedetti, C., Fallarino, F., et al. (2013). Tryptophan catabolites from microbiota engage aryl

Cell Host & Microbe
Clinical and Translational Report

CellPress

hydrocarbon receptor and balance mucosal reactivity via interleukin-22. Immunity *39*, 372–385. https://doi.org/10.1016/j.immuni.2013.08.003.

92. Venkatesh, M., Mukherjee, S., Wang, H., Li, H., Sun, K., Benechet, A.P., Qiu, Z., Maher, L., Redinbo, M.R., Phillips, R.S., et al. (2014). Symbiotic bacterial metabolites regulate gastrointestinal barrier function via the xenobiotic sensor PXR and toll-like receptor 4. Immunity *41*, 296–310. https://doi.org/10.1016/j.immuni.2014.06.014.

93. Illés, P., Krasulová, K., Vyhlídalová, B., Poulíková, K., Marcalíková, A., Pečinková, P., Sirotová, N., Vrzal, R., Mani, S., and Dvořák, Z. (2020). Indole microbial intestinal metabolites expand the repertoire of ligands and agonists of the human pregnane X receptor. Toxicol. Lett. *334*, 87–93. https://doi.org/10.1016/j.toxlet.2020.09.015.

94. Vyhlídalová, B., Krasulová, K., Pečinková, P., Marcalíková, A., Vrzal, R., Zemánková, L., Vančo, J., Trávníček, Z., Vondráček, J., Karasová, M., et al. (2020). Gut microbial catabolites of tryptophan are ligands and agonists of the aryl hydrocarbon receptor: A detailed characterization. Int. J. Mol. Sci. *21*, 2614. https://doi.org/10.3390/ijms21072614.

95. Gutiérrez-Vázquez, C., and Quintana, F.J. (2018). Regulation of the immune response by the aryl hydrocarbon receptor. Immunity *48*, 19–33. https://doi.org/10.1016/j.immuni.2017.12.012.

96. Safe, S., Jayaraman, A., and Chapkin, R.S. (2020). Ah receptor ligands and their impacts on gut resilience: structure–activity effects. Crit. Rev. Toxicol. *50*, 463–473. https://doi.org/10.1080/10408444.2020.1773759.

97. Cannon, A.S., Nagarkatti, P.S., and Nagarkatti, M. (2021). Targeting AhR as a novel therapeutic modality against inflammatory diseases. Int. J. Mol. Sci. *23*, 288. https://doi.org/10.3390/ijms23010288.

98. Duranton, F., Cohen, G., De Smet, R., Rodriguez, M., Jankowski, J., Vanholder, R., and Argiles, A.; on behalf of the European Uremic Toxin Work Group (2012). Normal and pathologic concentrations of uremic toxins. JASN *23*, 1258–1270. https://doi.org/10.1681/ASN.2011121175.

99. Tanaka, H., Sirich, T.L., and Meyer, T.W. (2015). Uremic solutes Produced by Colon Microbes. Blood Purif. *40*, 306–311. https://doi.org/10.1159/000441578.

100. Poesen, R., Windey, K., Neven, E., Kuypers, D., De Preter, V., Augustijns, P., D'Haese, P., Evenepoel, P., Verbeke, K., and Meijers, B. (2016). The influence of CKD on colonic microbial metabolism. J. Am. Soc. Nephrol. *27*, 1389–1399. https://doi.org/10.1681/ASN.2015030279.

101. Leclercq, S., Matamoros, S., Cani, P.D., Neyrinck, A.M., Jamar, F., Stärkel, P., Windey, K., Tremaroli, V., Bäckhed, F., Verbeke, K., et al. (2014). Intestinal permeability, gut-bacterial dysbiosis, and behavioral markers of alcohol-dependence severity. Proc. Natl. Acad. Sci. USA *111*, E4485–E4493. https://doi.org/10.1073/pnas.1415174111.

102. Reikvam, H., Hatfield, K., and Bruserud, Ø. (2016). The pretransplant systemic metabolic profile reflects a risk of acute graft versus host disease after allogeneic stem cell transplantation. Metabolomics *12*, 12. https://doi.org/10.1007/s11306-015-0880-x.

103. Turroni, F., Milani, C., Duranti, S., Ferrario, C., Lugli, G.A., Mancabelli, L., van Sinderen, D., and Ventura, M. (2018). Bifidobacteria and the infant gut: an example of co-evolution and natural selection. Cell. Mol. Life Sci. *75*, 103–118. https://doi.org/10.1007/s00018-017-2672-0.

104. Fujimura, K.E., Sitarik, A.R., Havstad, S., Lin, D.L., Levan, S., Fadrosh, D., Panzer, A.R., LaMere, B., Rackaityte, E., Lukacs, N.W., et al. (2016). Neonatal gut microbiota associates with childhood multisensitized atopy and T cell differentiation. Nat. Med. *22*, 1187–1191. https://doi.org/10.1038/nm.4176.

105. Fukuda, S., Toh, H., Hase, K., Oshima, K., Nakanishi, Y., Yoshimura, K., Tobe, T., Clarke, J.M., Topping, D.L., Suzuki, T., et al. (2011). Bifidobacteria can protect from enteropathogenic infection through production of acetate. Nature *469*, 543–547. https://doi.org/10.1038/nature09646.

106. Taur, Y., Jenq, R.R., Perales, M.-A., Littmann, E.R., Morjaria, S., Ling, L., No, D., Gobourne, A., Viale, A., Dahi, P.B., et al. (2014). The effects of intestinal tract bacterial diversity on mortality following allogeneic hematopoietic cell transplantation. Blood *124*, 1174–1182. https://doi.org/10.1182/blood-2014-02-554725.

107. Taur, Y., Xavier, J.B., LiPuma, L., Ubeda, C., Goldberg, J., Gobourne, A., Lee, Y.J., Dubin, K.A., Socci, N.D., Viale, A., et al. (2012). Intestinal domination and the risk of bacteremia in patients undergoing allogeneic hematopoietic stem cell transplantation. Clin. Infect. Dis. *55*, 905–914. https://doi.org/10.1093/cid/cis580.

108. Taur, Y., Coyte, K., Schluter, J., Robilotti, E., Figueroa, C., Gjonbalaj, M., Littmann, E.R., Ling, L., Miller, L., Gyaltshen, Y., et al. (2018). Reconstitution of the gut microbiota of antibiotic-treated patients by autologous fecal microbiota transplant. Sci. Transl. Med. *10*, eaap9489. https://doi.org/10.1126/scitranslmed.aap9489.

109. Holler, E., Butzhammer, P., Schmid, K., Hundsrucker, C., Koestler, J., Peter, K., Zhu, W., Sporrer, D., Hehlgans, T., Kreutz, M., et al. (2014). Metagenomic analysis of the stool microbiome in patients receiving allogeneic stem cell transplantation: loss of diversity is associated with use of systemic antibiotics and more pronounced in gastrointestinal graft-versus-host disease. Biol. Blood Marrow Transplant. *20*, 640–645. https://doi.org/10.1016/j.bbmt.2014.01.030.

110. Jenq, R.R., Taur, Y., Devlin, S.M., Ponce, D.M., Goldberg, J.D., Ahr, K.F., Littmann, E.R., Ling, L., Gobourne, A.C., Miller, L.C., et al. (2015). Intestinal *Blautia* is associated with reduced death from graft-versus-host disease. Biol. Blood Marrow Transplant. *21*, 1373–1383. https://doi.org/10.1016/j.bbmt.2015.04.016.

111. Shono, Y., Docampo, M.D., Peled, J.U., Perobelli, S.M., Velardi, E., Tsai, J.J., Slingerland, A.E., Smith, O.M., Young, L.F., Gupta, J., et al. (2016). Increased GVHD-related mortality with broad-spectrum antibiotic use after allogeneic hematopoietic stem cell transplantation in human patients and mice. Sci. Transl. Med. *8*, 339ra71. https://doi.org/10.1126/scitranslmed.aaf2311.

112. Peled, J.U., Gomes, A.L.C., Devlin, S.M., Littmann, E.R., Taur, Y., Sung, A.D., Weber, D., Hashimoto, D., Slingerland, A.E., Slingerland, J.B., et al. (2020). Microbiota as predictor of mortality in allogeneic hematopoietic-cell transplantation. N. Engl. J. Med. *382*, 822–834. https://doi.org/10.1056/NEJMoa1900623.

113. Markey, K.A., Schluter, J., Gomes, A.L.C., Littmann, E.R., Pickard, A.J., Taylor, B.P., Giardina, P.A., Weber, D., Dai, A., Docampo, M.D., et al. (2020). The microbe-derived short-chain fatty acids butyrate and propionate are associated with protection from chronic GVHD. Blood *136*, 130–136. https://doi.org/10.1182/blood.2019003369.

114. Lawley, B., Munro, K., Hughes, A., Hodgkinson, A.J., Prosser, C.G., Lowry, D., Zhou, S.J., Makrides, M., Gibson, R.A., Lay, C., et al. (2017). Differentiation of *Bifidobacterium longum* subspecies *longum* and *infantis* by quantitative PCR using functional gene targets. PeerJ *5*, e3375. https://doi.org/10.7717/peerj.3375.

115. Chalmers, N.I., Palmer, R.J., Cisar, J.O., and Kolenbrander, P.E. (2008). Characterization of a *Streptococcus* sp.- *Veillonella* sp. community micromanipulated from dental plaque. J. Bacteriol. *190*, 8145–8154. https://doi.org/10.1128/JB.00983-08.

116. Furet, J.-P., Firmesse, O., Gourmelon, M., Bridonneau, C., Tap, J., Mondot, S., Doré, J., and Corthier, G. (2009). Comparative assessment of human and farm animal faecal microbiota using real-time quantitative PCR. FEMS Microbiol. Ecol. *68*, 351–362. https://doi.org/10.1111/j.1574-6941.2009.00671.x.

117. Weisburg, W.G., Barns, S.M., Pelletier, D.A., and Lane, D.J. (1991). 16S ribosomal DNA amplification for phylogenetic study. J. Bacteriol. *173*, 697–703. https://doi.org/10.1128/jb.173.2.697-703.1991.

118. Djais, A.A., Theodorea, C.F., Mashima, I., Otomo, M., Saitoh, M., and Nakazawa, F. (2019). Identification and phylogenetic analysis of oral *Veillonella* species isolated from the saliva of Japanese children. F1000Res *8*, 616. https://doi.org/10.12688/f1000research.18506.5.

119. Al-Ghalith, G., and Knights, D. (2020). BURST enables mathematically optimal short-read alignment for big data. https://doi.org/10.1101/2020.09.08.287128.

120. McMurdie, P.J., and Holmes, S. (2013). phyloseq: an R package for Reproducible Interactive Analysis and Graphics of microbiome Census Data. PLoS One *8*, e61217. https://doi.org/10.1371/journal.pone.0061217.

121. Fernandes, A.D., Macklaim, J.M., Linn, T.G., Reid, G., and Gloor, G.B. (2013). ANOVA-like differential expression (ALDEx) analysis for mixed population RNA-seq. PLoS One 8, e67019. https://doi.org/10.1371/journal.pone.0067019.

122. Harrison, E., Drake, T., and Ots, R. (2002). Finalfit: quickly create elegant regression results tables and plots when modelling R package version 1.0.53. https://finalfit.org/.

123. Bittinger, K. (2017). Usedist: Distance Matrix Utility. https://github.com/kylebittinger/usedist.

124. Dixon, P. (2003). VEGAN, a package of R functions for community ecology. J. Veg. Sci. 14, 927–930. https://doi.org/10.1111/j.1654-1103.2003.tb02228.x.

125. Martinez, A. (2020). pairwiseAdonis: pairwise multilevel comparison using adonis R package version 0.4. https://github.com/pmartinezarbizu/pairwiseAdonis.

126. Han, J., Lin, K., Sequeira, C., and Borchers, C.H. (2015). An isotope-labeled chemical derivatization method for the quantitation of short-chain fatty acids in human feces by liquid chromatography–tandem mass spectrometry. Anal. Chim. Acta 854, 86–94. https://doi.org/10.1016/j.aca.2014.11.015.

127. Evans, A., Bridgewater, B., Liu, Q., Mitchell, M., Robinson, R., Dai, H., Stewart, S., DeHaven, C., and Miller, L. (2014). High resolution mass spectrometry improves data quantity and quality as compared to unit mass resolution mass spectrometry in high-throughput profiling metabolomics. Metabolomics 4, 1000132. https://doi.org/10.4172/2153-0769.1000132.

128. Montero-Pau, J., Gómez, A., and Muñoz, J. (2008). Application of an inexpensive and high-throughput genomic DNA extraction method for the molecular ecology of zooplanktonic diapausing eggs: rapid DNA extraction for diapausing eggs. Limnol. Oceanogr.: Methods 6, 218–222. https://doi.org/10.4319/lom.2008.6.218.

Cell Host & Microbe
Clinical and Translational Report

 CellPress

STAR★METHODS

KEY RESOURCES TABLE

REAGENT or RESOURCE	SOURCE	IDENTIFIER
Bacterial and virus strains		
Bifidobacterium longum subspecies *infantis*	*B. infantis* isolate that shares >99.9% nucleotide identity with the *B. infantis* type strain (ATCC 15697)	PBI001
Bifidobacterium longum subspecies *infantis*	Button et al.[24]; isolated from a commercially available probiotic	PLMB0001
Veillonella parvula	American Type Culture Collection (Manassas, VA)	ATCC 10790
Veillonella sp.	This study	PL001
Veillonella rogosae	This study	PL002
Biological samples		
Donor-derived human milk oligosaccharides (HMO) concentrate	This study	N/A
Chemicals, peptides, and recombinant proteins		
Brucella Blood agar	Anaerobe Systems	Cat#AS-141
Reinforced Clostridial Medium	BD Difco	Cat#218081
Lactobacilli MRS Broth	BD Difco	Cat#288130
Beef extract	Hardy	Cat#C5100
Yeast extract	Gibco	Cat#212750
Peptone	Gibco	Cat#211677
2-(N-morpholino)ethanesulfonic acid (MES)	Sigma	Cat#69892
Sodium chloride	Sigma	Cat#S3104
Cysteine hydrochloride	Sigma	Cat#7880
Hemin	Sigma	Cat#51280
Menadione	Sigma	Cat#M5625
ATCC vitamin supplement	American Type Culture Collection	Cat#MD-VS
ATCC trace mineral supplement	American Type Culture Collection	Cat#MD-TMSC
Sodium lactate	Sigma	Cat#L4263
Critical commercial assays		
Exo-SapIT	Applied Biosystems/ ThermoFisher	Cat# 78201.1.ML
ZymoBiomics 96 MagBead DNA Kit (Lysis Tubes)	Zymo Research, Inc.	Cat#D4308
Applied Biosystems™ TaqMan™ Fast Advanced Master Mix	ThermoFisher Scientific	Cat # 4444556
Deposited data		
Whole metagenomic sequencing data	This study; NCBI Sequencing Read Archive	BioProject: PRJNA993161
Experimental models: Organisms/strains		
Mouse: C57BL/6NTac (Germ-free)	Taconic Biosciences	Model#GF-B6-F; RRID: IMSR_TAC:b6
Oligonucleotides		
B. infantis-specific sialidase; forward primer 5'-ATACAGCAGAACCTTGGCCT	Lawley et al.[114]	N/A
B. infantis-specific sialidase; reverse primer 5'-GCGATCACATGGACGAGAAC	Lawley et al.[114]	N/A

(Continued on next page)

Continued

REAGENT or RESOURCE	SOURCE	IDENTIFIER
B. infantis-specific sialidase; probe 5'-FAM/TTTCACGGA/ZEN/TCACCGG ACCATACG-3IABkFQ	Lawley et al.[114]	N/A
Veillonella 16S rRNA; forward primer 5'-CCGTGATGGGATGGAAACTGC	Chalmers et al.[115]	N/A
Veillonella 16S rRNA; reverse primer 5'-CCT TCG CCA CTG GTG TTC TTC	Chalmers et al.[115]	N/A
Eubacterium 16S rRNA; forward primer 5'-CGGTGAATACGTTCCCGG	Furet et al.[116]	N/A
Eubacterium 16S rRNA; reverse primer 5'-TACGGCTACCTTGTTACGACTT	Furet et al.[116]	N/A
Universal 16S 27F 5'-AGAGTTTGATYMTGGCTCAG	Weisburg et al.[117]	N/A
Universal 16S 1492R 5'-GTTTACCTTGTTACGACTT	Weisburg et al.[117]	N/A
Veillonella rpoB; forward primer 5'-GTAACAAAGGTGTCGTTTCTCG	Djais et al.[118]	N/A
Veillonella rpoB; reverse primer 5'-GCA CCR TCA AAT ACA GGT GTA GC	Djais et al.[118]	N/A
Software and algorithms		
GraphPad Prism	GraphPad Software; Version 9.0.2 or higher	https://www.graphpad.com/scientific-software/prism/
BURST	Al-Ghalith and Knights[119]	https://github.com/knights-lab/BURST
R package *phyloseq* (v1.41.0)	McMurdie and Holmes[120]	https://www.bioconductor.org/packages/release/bioc/html/phyloseq.html
R package *ALDEx2* (v1.29.1)	Fernandes et al.[121]	https://bioconductor.org/packages/release/bioc/html/ALDEx2.html
R package *finalfit* (v1.0.5)	Harrison et al.[122]	https://finalfit.org/
R package *usedist* (v0.4.0)	Bittinger[123]	https://github.com/kylebittinger/usedist
R package *vegan* (v2.6-2)	Dixon[124]	https://github.com/vegandevs/vegan
R package *pairwiseAdonis* (v0.4)	Martinez[125]	https://github.com/pmartinezarbizu/pairwiseAdonis
Other		
Sanger sequencing	Azenta Life Sciences	https://www.genewiz.com/en/Public/Services/Sanger-Sequencing
Short chain fatty acid quantification	Precion	https://www.precion.com/services/short-chain-fatty-acid/
Untargeted global metabolomics platform	Metabolon	https://www.metabolon.com/solutions/global-metabolomics/
Serum metabolite quantification	Precion	https://www.precion.com/services/metabolite-profiling/
BoosterShot shallow shotgun metagenomic sequencing	Diversigen	https://www.diversigen.com/services/boostershot/

RESOURCE AVAILABILITY

Lead contact

Further information and requests for resources and reagents should be directed to and will be fulfilled by the lead contact, Gregory McKenzie (gmckenzie@prolacta.com).

Cell Host & Microbe
Clinical and Translational Report

CellPress

Materials availability

HMO concentrate will be provided under a material transfer agreement depending upon product availability. Bacterial isolates generated during this study will be provided under a material transfer agreement.

Data and code availability

- Raw whole metagenomic sequencing data derived from human samples are deposited at the NCBI Sequencing Read Archive (SRA) and will be made publicly available by the date of publication.
- Metabolomics data derived from human samples are available in Table S5.
- *In vivo* and *in vitro* data reported in this paper will be shared by the lead contact upon request.
- This paper does not report original code.
- Any additional information required to reanalyze the data reported in this paper is available from the lead contact upon request.

EXPERIMENTAL MODEL AND SUBJECT DETAILS

Human subjects

Table S1 reports metadata, including age and sex, corresponding to the 56 healthy adult subjects enrolled in an unblinded study (clinicaltrials.gov ID NCT05141903). This study was reviewed and approved by Alpha IRB, an independent IRB located in Costa Mesa, CA. All subjects were provided with an explanation of the study and gave informed consent in writing prior to the start of their participation in the study.

Murine studies

In vivo studies used singly-housed germ-free female C57BL/6 mice (age 5-6 weeks, Taconic) maintained on Teklad Global Rodent Diet 2918. Animals were housed in a positive-pressure clean room with HEPA filtration (bioBubble) in solid-bottom micro-isolator cages (Innovive Innocage MVX6 with M-feed food hoppers), given sterile water *ad libitum* (Innovive Aquavive M-WB-300A), and provided with sterile 1/8" corn cob bedding (Teklad 7902). Environmental conditions were maintained at 20-26°C, humidity 30-70%, with a 12/12 hour light/dark cycle. Health checks were performed at least twice daily and included observation of behavior and appearance. Animal work was carried out in accordance with the recommendations in the Guide for the Care and Use of Laboratory Animals of the National Institutes of Health. All protocols were approved by the TransPharm PreClinical Solutions Institutional Animal Care and Use Committee. For additional study details, see "method details" section.

Bacterial strains and growth conditions

The *Bifidobacterium longum* subspecies *infantis* strain PBI001 used in *in vitro* co-culture and murine studies is an isolate that shares >99.9% nucleotide identity with the *B. infantis* type strain ATCC 15697. For determination of antibiotic susceptibility, *B. infantis* was isolated from the commercially available probiotic that was used in the human study and designated as PLMB0001. *B. infantis* strains were propagated at 37°C anaerobically on Reinforced Clostridial Medium (RCM, BD Difco # 218081), lactobacilli MRS Broth (BD Difco # 288130), and Brucella Blood agar (BRU, Anaerobe Systems AS-141). *Veillonella parvula* ATCC 10790 was acquired from the American Type Culture Collection and two additional strains of *Veillonella*, PL001 and PL002, were isolated from subjects in the *B. infantis* + HMO cohort of this study. All *Veillonella* were propagated anaerobically at 37°C in liquid Reinforced Clostridial Media (RCM) with 60% sodium lactate and on Brucella Blood agar (BRU, Anaerobe Systems AS-141).

METHOD DETAILS

Healthy human subject study methods

Two hundred and twenty-four healthy adult subjects were initially screened for suitability (see inclusion and exclusion criteria used to evaluate subject suitability listed below). Ninety-two of the subjects were then enrolled in an unblinded, multi-dose study (clinicaltrials.gov ID NCT05141903) designed to test multiple hypotheses. This publication focused on results from three cohorts (n=56 subjects, Table S1) and addressed a subset of the hypotheses: that *B. infantis* and HMO treatment influence microbiome recovery after antibiotics, and that antibiotic treatment enhances *B. infantis* engraftment. This study was reviewed and approved by Alpha IRB, an independent IRB located in Costa Mesa, CA. All subjects were provided with an explanation of the study and gave informed consent in writing prior to the start of their participation in the study. Eligibility for enrollment was determined by screening samples of blood, urine, and stool for markers of health and for the absence of vancomycin-resistant enterococci and *C. difficile*.

Inclusion criteria were:

- Healthy adults between the ages of 18-75 years (required at the time of consent) who can provide proof of vaccination against SARS-CoV-2. Proof may be a physical or electronic record of vaccination or self-attestation (to include approximate vaccination date and manufacturer of vaccine) if a copy of the vaccination record is not available
- Subjects must have a BMI of 18 - 30 at screening visit
- Willingness to complete study specific questionnaires

- Willingness to complete journal to record investigational product (IP) dosing times, Bristol stool scores, and IP flavor questionnaires
- Willingness to complete all study procedures, clinic visits, and provide required biospecimen samples
- Willingness to collect and process stool samples at home and transport stool samples to clinic
- Sexually active females of child-bearing potential must agree to use highly effective methods of contraception during heterosexual intercourse throughout the study period and for three days following discontinuation of IP, whichever comes later. Examples of highly effective methods include the use of two forms of contraception with one being an effective barrier method (e.g., a condom and spermicide used together), or have a vasectomised partner. Abstinence is acceptable as a life-style choice. Female subjects who utilize hormonal contraceptives as one of their birth control methods must have used the same method for at least 3 months before study dosing
- Provide informed consent

Exclusion criteria were:

- Subjects with a BMI of 17 or less or 31 or greater are excluded
- Women who are pregnant or breastfeeding, or intend to become pregnant during the course of this study
- Subjects who intend to take a probiotic during the study
- Subjects with self-reported diarrhea on day 1 prior to dosing, whereby diarrhea is defined as two or more episodes of watery and/or unformed stool within 24 hours
- Alcohol or drug abuse during the last 12 months, including failing a screen for drugs of abuse at screening and day 1 of the study
- Unstable medical condition, in the opinion of the investigator
- Subject with a history of allergy to vancomycin and/or metronidazole
- Clinically significant abnormal laboratory test results at screening
- Subjects who are unable or unwilling to provide stool samples on a regular basis as per study protocol
- Participation in a clinical research trial within 30 days prior to screening
- Unable to give informed consent
- Any condition which may preclude subject's ability to comply with and complete the study or may pose a risk to the health of the subject
- Known carriers of *C. difficile* prior to study start, as determined by qPCR of stool
- Known carriers of vancomycin-resistant enterococci (VRE) prior to study start, as determined by stool culture
- Subjects with history of lactose intolerance

Subjects were assigned into 5 cohorts of 18 subjects each. The randomization scheme for this study was as follows. The first twenty subjects were randomized into the antibiotics only control or *B. infantis* + HMO cohorts using a randomized permuted block scheme. The next thirty-four subjects were randomized into the antibiotics only control, *B. infantis* + HMO, and *B. infantis* only cohorts using a similar separate randomized permuted block scheme employing a 4:4:9 ratio in blocks of 17. Four of the subjects terminated their participation in the study early, and two of these, both receiving only the antibiotics, were replaced. One of the four subjects who terminated early, belonging to the antibiotics only cohort, withdrew after their day 14 sample was provided and was therefore included in analyses. Of the four that withdrew, one had scheduling conflicts and could not attend the clinic for blood and stool sampling as required, one provided no reason for withdrawal of consent, and two withdrew consent because of an adverse event unrelated to the product. None were terminated for safety-related reasons.

Cohort treatment regimens are as follows. Briefly, one cohort received antibiotics alone, one cohort received antibiotics and a commercially available *B. infantis* probiotic, and the remaining cohort was dosed with antibiotics, the *B. infantis* probiotic, and 18 g/day HMO. Subjects received 250 mg vancomycin and 500 mg of metronidazole three times per day on days 1-5. Subjects receiving *B. infantis* were given 8×10^9 colony-forming units (CFU) per oral dose of a commercially available probiotic once a day from days 1–14. HMO was prepared as described below and given to subjects orally in liquid form twice a day from days 1–28. Stool samples were collected during eligibility screening and on days 1, 3, 4, 5, 7, 9, 11, 14, 17, 21, 28, and 35, where day 1 was the first day of the protocol. Some subjects were asked to return to the study site and provide a stool sample on or after day 90. Blood samples were also drawn on days 1, 5, 14, 28 and 35, processed to serum, and frozen. On study days 1, 5, 9, 14, 28, and 35, stool was refrigerated at 4°C after production and frozen at -80°C within 24 hours. On days 3, 4, 7, 11, 17, and 21 of the study, a portion of each stool was preserved in ethanol immediately after production and frozen at -80°C within one week.

Preparation of HMO Concentrate
The HMO concentrate used in the human study and in *in vivo* and *in vitro* experiments was manufactured by Prolacta Bioscience (Duarte, CA). Prolacta Bioscience makes human milk nutritional products from donated breast milk, intended for use by extremely premature infants in the neonatal intensive care unit, and by term infants born with congenital malformations requiring immediate surgery. The milk is obtained from healthy donors who produce excess milk beyond the needs of their own infants. The donors are carefully screened for a variety of infectious diseases and lifestyle elements, such as drug use including nicotine, similar to what occurs in a blood bank. All potential donors provide attestation from their baby's pediatrician that the baby will not be adversely affected if the mother donates her excess breast milk. Individual milk donations are also screened for a variety of pathogens of

Cell Host & Microbe
Clinical and Translational Report

CellPress

concern. All donors sign informed consent as part of their contract with Prolacta prior to donation and are aware that a portion of their milk may be used for the development of new products or other research purposes. Multiple lots of pooled human milk, from up to 200 donors per lot, were used to prepare the HMO product. Human milk permeate, a by-product of ultrafiltration used during the manufacture of commercial human milk-based human milk fortifier and ready-to-feed products (Prolacta Bioscience, Duarte, CA), consists primarily of water, lactose, HMO, and minerals. HMO concentrate was generated by subsequently removing lactose from the permeate and carrying out further ultrafiltration and pasteurization steps. The test product was supplied as a frozen liquid, stored at $\leq$-20°C, and thawed prior to administration.

Determination of pH of human stool
For the determination of the pH of neat feces, approximately 100 mg of feces were suspended in 100 μL HPLC grade water, thoroughly mixed, and centrifuged. The supernatant was applied to narrow range pH strips (pH 4.5-9.0, life2o).

DNA extraction from human stool, quantification, and *B. infantis*-specific qPCR
Genomic DNA was extracted from frozen neat stools or stools preserved in ethanol using ZymoBiomics™ 96 MagBead DNA kits (Zymo Research) following the manufacturer's instructions. The concentration of the extracted DNA was measured on a Nanodrop 8000 (Thermo Scientific). To quantify *B. infantis* in stool samples, qPCR was performed with primers specific to a *B. infantis* sialidase gene, as previously described.[114] Oligonucleotides are listed in the key resources table. The qPCR assay composition consisted of Applied Biosystems™ TaqMan™ Fast Advanced Master Mix (ThermoFisher), 10 μM forward and 10 μM reverse primers (IDT), 10 μM probe (IDT), and molecular biology grade water (Fisher). Sample DNA was added to reach a final concentration of 3 ng in the reaction. The final reaction volume for the qPCR assay was 10 μL. All reactions were run in 384-well Applied Biosystems™ MicroAmp Optical Reaction plates (ThermoFisher) and sealed with Applied Biosystems™ MicroAmp Optical adhesive films (ThermoFisher). Samples were run in triplicate. Experiments were run on an Applied Biosystems™ QuantStudio 5 Real-Time PCR machine (ThermoFisher) using the following assay conditions: initial activation of the polymerase at 50°C for two minutes and 95°C for 30 seconds, followed by 40 cycles of 95°C for 10 seconds, then 60°C for 30 seconds. Analysis was performed using Applied Biosystems™ QuantStudio Design & Analysis Software v1.5.2 and reported as gene copies per nanogram of DNA.

Quantification of short-chain fatty acids and lactate in human stool
Stool samples from days 1, 5, 9, 11, 14, 17, 28, and 35 were sent to Precion, Ltd. (Morrisville, NC) for extraction and analysis. A portion of a neat sample was transferred into a 2 mL cryotube containing three stainless steel 1/8" cone balls, and the exact weight of the sample was recorded. A solution of deuterium-labelled internal standards in water (50 μL) and 1.5 mL of methanol was added to the cryotube and the sample was homogenized by vortex-mixing for 2 minutes. Alternatively, ethanol-preserved stool samples were centrifuged and 50 μL of the supernatant was transferred to a 2 mL cryotube together with 50 μL standards and 1.0 mL methanol, and vortex-mixed for 2 minutes. The resulting suspensions were centrifuged at 2,000 x *g* at 20°C for 10 minutes, and 50 μL of the supernatant was transferred to a 96-well plate and derivatized using a modified version of the published protocol.[126] An aliquot of the reaction mixture was analyzed by liquid-chromatography mass spectrometry (LC-MS/MS) using an Exion UHPLC (Sciex) coupled to a 5500+ Triple Quadrupole Mass Spectrometer (Sciex) in ESI negative mode using a C18 column (Zorbax Eclipse plus C18 1.8 micron, 2.1x50 mm, Agilent). The peak areas of the respective parent to product ion transitions were measured against the peak area of the parent to product ion transitions of the corresponding labelled internal standards for the quantitated metabolites. Quantitation was performed with Sciex OS-MQ software (Sciex) based on fortified calibration standards prepared immediately prior to each run.

For neat stool samples, raw data were weight corrected to account for the individual wet weight of each sample providing the analyte content in μg/g wet weight. Additionally, using a separate sample aliquot, the dry weight/wet weight ratio was determined for each sample and each dry weight/wet weight ratio was used to calculate the analyte content of each sample in μg/g dry weight. For ethanol-preserved samples, raw data were weight corrected to account for the individual dry weight of each sample. Using a separate sample aliquot (750 μL sample suspension), the dry weight/volume ratio was determined for each sample. Each dry weight/volume ratio was used to calculate the analyte content of each sample in μg/g dry weight. Data were then transformed to mmol/kg by dividing by the molecular weight of the analyte.

Quantification of metabolites in human serum
Serum samples from days 1, 5, 14, 28, and 35 were analyzed quantitatively by LC-MS/MS for 70 analytes at Precion Ltd., Morrisville, NC, USA. This analysis consisted of two extractions of the serum samples. To the first extraction (100 μL), a solution of stable labelled internal standards was added followed by protein precipitation. After centrifugation, one portion of the supernatant was removed, evaporated to dryness, reconstituted and an aliquot analyzed on a Sciex Exion LC/Sciex 5500+ Triple Quadrupole Mass Spectrometer LC-MS/MS system in ESI negative mode using C18 reversed phase chromatography. This assay covered organic acids, phenolic compounds, sulfates, and other analytes that are negatively charged under negative ESI mass spectrometer conditions. A second portion of the supernatant was removed, evaporated to dryness, reconstituted, and an aliquot analyzed on a Sciex Exion LC/Sciex 5500+ Triple Quadrupole Mass Spectrometer LC-MS/MS system in ESI positive mode using C18 reversed phase chromatography. This analysis covered amino acids, amines, and other analytes that were positively charged under positive ESI mass spectrometer conditions.

A second extraction was performed from 50.0 μL of the serum sample. A solution of stable labelled internal standards was added to serum samples followed by protein precipitation. After centrifugation, a portion of the supernatant was removed and derivatized with a substituted hydrazine to form the corresponding acid hydrazides of short chain fatty acids. An aliquot of the resulting mixture was analyzed on a Sciex Exion LC/Sciex 5500+ Triple Quadrupole Mass Spectrometer LC-MS/MS system in ESI positive mode using C18 reversed phase chromatography.

For all methods, the peak areas of the respective parent to product ion transitions were measured against the peak areas of the parent to product ion transitions of the corresponding labelled internal standards. Stable labelled versions of each of the 70 analytes were used as internal standards. Quantitation was performed using a weighted linear least squares regression analysis generated from fortified calibration standards (6 to 10 concentration levels, depending on analyte) prepared concurrently with study samples and quality control samples in each analytical run.

Global metabolomics analysis of human stool

Untargeted metabolomic profiling was performed on stool samples from days 1, 5, and 14 at Metabolon, Inc (Morrisville, NC, USA) using a combination of LC-MS methods as described.[127] All methods utilized a Waters ACQUITY UPLC and a Thermo Scientific Q-Exactive high resolution/accurate mass spectrometer interfaced with a heated electrospray ionization (HESI-II) source and Orbitrap mass analyzer operated at 35,000 mass resolution. Briefly, the sample extract was dried then reconstituted in solvents compatible to each of the four methods. Each reconstitution solvent contained a series of standards at fixed concentrations to ensure injection and chromatographic consistency. Based on Metabolon, Inc protocols and previously published methods, the first aliquot was analyzed using acidic positive ion conditions, chromatographically optimized for more hydrophilic compounds. The second aliquot was also analyzed using acidic positive ion conditions; however, it was chromatographically optimized for more hydrophobic compounds. The third aliquot was analyzed using basic negative ion optimized conditions and a separate dedicated C18 column. The fourth aliquot was analyzed via negative ionization following elution from a HILIC column (Waters UPLC BEH Amide 2.1 × 150 mm, 1.7 μm) using a gradient consisting of water and acetonitrile with 10 mM Ammonium Formate, pH 10.8. The MS analysis alternated between MS and data-dependent MS^n scans using dynamic exclusion. The scan range varied slighted between methods but covered 70–1000 m/z.

Raw data were extracted, peak-identified, and QC processed using Metabolon's hardware and software. These systems are built on a web-service platform utilizing Microsoft's .NET technologies, which run on high-performance application servers and fiber-channel storage arrays in clusters to provide active failover and load-balancing. Compounds are identified by comparison to library entries of purified standards or recurrent unknown entities. Metabolon maintains a library based on authenticated standards that contains the retention time/index (RI), mass to charge ratio (m/z), and chromatographic data (including MS/MS spectral data) on all molecules present in the library. Furthermore, biochemical identifications are based on three criteria: retention index within a narrow RI window of the proposed identification, accurate mass match to the library +/- 10 ppm, and the MS/MS forward and reverse scores. MS/MS scores are based on a comparison of the ions present in the experimental spectrum to ions present in the library entry spectrum. While there may be similarities between these molecules based on one of these factors, the use of all three data points can be utilized to distinguish and differentiate biochemicals. More than 4500 commercially available purified standard compounds have been acquired and registered into a database for analysis on all platforms for determination of their analytical characteristics. Additional mass spectral entries have been created for structurally unnamed biochemicals, which have been identified by virtue of their recurrent nature (both chromatographic and mass spectral). These compounds have the potential to be identified by future acquisition of a matching purified standard or by classical structural analysis.

Metabolites were identified by comparison to a referenced library of chemical standards, and area-under-the-curve analysis was performed for peak quantification and normalized to day median value. To ensure high quality of the dataset, control and curation processes were subsequently used to ensure true chemical assignment and remove artifacts and background noise. Metabolites were scaled by run-day medians and log-transformed before statistical analysis. Two-way repeated measures ANOVA contrasts were used to analyze the data. For all analyses, missing values, if any, were imputed with the observed minimum for that compound. The statistical analyses were performed on natural log-transformed data using ArrayStudio.

Whole metagenomic sequencing and analyses

DNA extracted from human stool samples from days 1, 5, 9, 14, 28, and 35 as described above was used to prepare libraries for shotgun metagenomic sequencing, and paired-end sequencing (2 x 150 bp) was performed on an Illumina NovaSeq instrument to generate a target of ∼2 million reads per sample (BoosterShot, Diversigen Inc.).

Sequence analyses followed an established pipeline (Diversigen Inc.). Briefly, sequences were aligned to a curated database containing all representative genomes in RefSeq for bacteria with additional manually curated strains. Alignments were made at 97% identity against all reference genomes. Every input sequence was compared to every reference sequence in the Diversigen Venti database using fully gapped alignment with BURST.[119] Ties were broken by minimizing the overall number of unique Operational Taxonomic Units (OTUs). For taxonomy assignment, each input sequence was assigned the lowest common ancestor that was consistent across at least 80% of all reference sequences tied for best hit. Samples with fewer than 10,000 sequences were discarded. OTUs accounting for less than one millionth of all strain-level markers and those with less than 0.01% of their unique genome regions covered (and < 0.1% of the whole genome) at the species level were discarded. The counts for each OTU in this filtered table were normalized to the OTU's genome length, and filtered tables for the normalized counts and relative abundance of each OTU were

Cell Host & Microbe
Clinical and Translational Report

CellPress

generated. Strain-level tracking, including for *B. infantis*, used the "capitalist" algorithm in BURST to assign reads to genomes in the Diversigen Venti database. Rather than applying a lowest common ancestor approach, the "capitalist" algorithm returns a minimal set of genomes that can explain all the reads in a sample. From that output, an OTU table was calculated with the read counts per genome per sample. Alpha diversity metrics (observed reads and Shannon diversity) were calculated using the filtered OTU table rarefied to a read depth of 76,000 using the R package *phyloseq* (v.1.41.0).[120] Bray-Curtis dissimilarity was calculated on the same filtered data, aggregated at the genus taxonomic level and rarefied to 76,000 reads using the R package *phyloseq* (v1.41.0). The filtered OTU table aggregated at the Family taxonomic level was used to calculate the top Families among cohorts. All taxa >1% abundance in any cohort were kept and all taxa <1% among taxa were grouped into an "Other" category. The count table of aggregated genera was then centered log-ratio (CLR) transformed by taking the median CLR value for each OTU sampled 150 times from a Dirichlet model using the R package *ALDEx2* (v.1.29.1).[121]

Determination of the susceptibility of *B. infantis* to vancomycin and metronidazole

Susceptibility of *B. infantis* PLMB0001 to vancomycin and metronidazole was determined by the Special Studies Laboratory at Tufts Medical Center according to guidelines set by the Clinical and Laboratory Standards Institute (CLSI). In brief, *B. infantis* PLMB0001 was subcultured by purity streaking onto Centers for Disease Control (CDC) anaerobic blood agar (ABA) (Remel Products, Lenexa, KS) for at least two serial transfers, and then a 48-hr culture was resuspended to a MacFarland standard of 0.5 and spotted onto Supplemented Brucella Agar (BD BBL, Franklin Lakes, NJ) containing laked sheep blood (Hemostat Laboratories, Dixon, CA) (5% v/v) and either vancomycin or metronidazole at various concentrations. Serial two-fold dilutions of each antibiotic were tested, ranging from 0.06–128 μg/mL for vancomycin and 0.12–32 μg/mL for metronidazole. The minimum inhibitory concentrations (MICs) of each antibiotic were interpreted using standards set by CLSI.

Culturing and isolation of *Veillonella* strains

Bacterial strains PL001 and PL002 were isolated from fecal samples of subjects in the *B. infantis* + HMO cohort. The fecal samples had been previously preserved at -80ºC, and an aliquot was thawed and serially diluted into anoxic filter-sterilized PBS (pH 7.0). Aliquots of serial dilutions were plated onto pre-reduced Brucella Blood Agar (Anaerobe Systems). Plates were incubated anaerobically at 37°C for 2-5 days. Individual colonies were picked, arrayed onto a fresh plate of the same agar, and regrown for 2-5 days. DNA was extracted from the arrayed isolates using an alkaline lysis buffer technique[128] and the bacterial 16S rRNA gene was amplified by PCR using the established universal 16S primers 27F and 1492R.[117] The PCR products were cleaned using Exo-SapIT (Applied Biosystems) and two-directional Sanger sequencing was performed using the same primers to assign taxonomic identity to each strain (Azenta Life Sciences).

Under anaerobic conditions, pure cultures of arrayed isolates identified as *Veillonella* were prepared by picking and streaking onto fresh media three times. A single colony was inoculated into 30 mL of liquid Reinforced Clostridial Media (RCM) with 60% sodium lactate, and the culture was grown anaerobically at 37°C for 1-3 days. The cell culture was mixed with pre-reduced glycerol and PBS to a final concentration of 15% glycerol, aliquots were distributed to cryovials, and the cryovials were frozen and stored at -80°C. The same culturing conditions were used to propagate and bank *V. parvula* ATCC 10790, after initial revival from a lyophilized stock by streaking onto BRU.

PL001 and PL002 were subjected to PCR and Sanger sequencing using the 16S rRNA primers described above and primers specific to the *Veillonella rpoB* gene (see the key resources table), with resulting sequences aligned to known *Veillonella* sequences to assign specific species identity. PL001 was highly similar to *V. infantium*, *V. dispar*, and *V. nakazawae*, and species identity could not be definitively assigned based on *rpoB* or 16S sequences. PL002 was identified as *V. rogosae*.

Assessment of growth and SCFA production of *Veillonella* strains during growth on lactate and co-culture with *B. infantis*

Frozen glycerol stocks (*V*. sp. PL001, *V. rogosae* PL002, *V. parvula* ATCC 10790) were used to inoculate cultures at 1 x 10^5 CFU/mL. *B. infantis* PBI001 was inoculated at 1 x 10^4 CFU/mL. Assay media was a modification of reinforced clostridial medium and contained 7.5 g/L bacto peptone (Gibco 211677), 7.5 g/L beef extract (Hardy C5100), 2.25 g/L yeast extract (Gibco 212750), 18.65 g/L 2-(N-morpholino)ethanesulfonic acid (MES) (Sigma 69892), 5 g/L sodium chloride (Sigma S3104), 0.55 g/L cysteine hydrochloride (Sigma C7880), 1 mg/L hemin (Sigma 51280), 1 mg/L menadione (Sigma M5625), 10 mL/L ATCC vitamin supplement (ATCC MD-VS), and 10 mL/L ATCC trace mineral supplement (ATCC MD-TMSC), adjusted to pH 6.8. As indicated in figure legends, media was supplemented with 0.01-1% sodium lactate (Sigma L4263), 0.25% monosaccharide-depleted HMO concentrate, or no additional carbon source. For co-culture experiments, bacteria were cultured in 1 mL volumes in deep-well 96-well plates and incubated anaerobically at 37°C. For lactate titration experiments, bacteria were cultured in 200 μL volumes in flat-bottomed microtiter plates with liquid reservoirs and incubated anaerobically at 37°C in a spectrophotometer, taking OD600 readings every 30 minutes. After 30 hours of incubation, triplicate cultures were pooled, and 400 μL of pooled culture was frozen and used for quantification of metabolites. A 200 μL aliquot of pooled culture was used to extract DNA using the ZymoBiomics 96 MagBead DNA Kit (Zymo Research, Inc). Extracted DNA was used to enumerate copy number of *B. infantis* via qPCR of the sialidase gene as described above, as well as copy number of *Veillonella* via SYBR-green-based qPCR of the 16S gene employing primers listed in the key resources table.

Murine model of *B. infantis* engraftment

Frozen glycerol stocks of *V. parvula* were generated as described above. *B. infantis* PBI001was propagated for mouse studies in Reinforced Clostridial Medium (RCM, BD Difco # 218081) or lactobacilli MRS Broth (BD Difco # 288130). Cultures were centrifuged, and cell pellets were resuspended in phosphate-buffered saline (PBS) with glycerol at a final concentration of 15%, aliquoted, and frozen at -80°C for long term storage. Viable colony-forming units (CFU) were determined by diluting and plating onto Brucella Blood Agar (Anaerobe Systems AS-141) and growing anaerobically at 37°C.

Singly-housed germ-free female C57BL/6 mice (age 5-6 weeks, Taconic) were inoculated with 1 x 10^7 colony-forming units *V. parvula* ATCC 10790 or *B. infantis*. After a 7-day stabilization period, *V. parvula*-associated animals were orally gavaged with sterile phosphate buffered saline (PBS) or 1 x 10^8 CFU of *B. infantis* resuspended in 0.2 mL of HMO concentrate (100 g/L). *B. infantis*-associated animals were gavaged with 0.2 mL HMO concentrate (100g/L). For the following three days, animals were gavaged once daily with PBS or HMO concentrate. Three hours after the final gavage, animals were humanely euthanized by CO_2 asphyxiation followed by cardiac exsanguination, and tissues were immediately harvested. Contents of the ileum, cecum, and rectum were squeezed into a sterile vial and immediately snap-frozen for analysis of short-chain fatty acids and lactate. Cage bottom fecal samples were collected from each individual animal throughout the study and frozen. DNA extraction from fecal pellets was performed using the ZymoBiomics 96 MagBead DNA Kit (Zymo Research, Inc). To quantify *B. infantis* in fecal samples, qPCR was performed as previously described. *V. parvula* abundance in fecal samples was quantified using qPCR as described above. One of the eighteen mice associated with *V. parvula* did not exhibit detectable *Veillonella* signal after the 7-day stabilization period and was excluded from the remainder of the study.

Quantification of short-chain fatty acids and lactate in mouse cecal contents and *in vitro* supernatants

Frozen mouse cecal contents were thawed and approximately 100 mg of material was transferred into a 2 mL cryotube containing three stainless steel 1/8" cone balls, and the exact weight of the sample was recorded. A solution of deuterium-labelled internal standards in water (50 μL) and 1.5 mL of methanol was added to the cryotube and the sample was homogenized by vortex-mixing for 2 minutes. Alternatively, frozen bacterial cultures were thawed, centrifuged to pellet cells, and 50 μL of supernatant transferred to a 2 mL cryotube together with 50 μL standards and 1.0 mL methanol, and vortex-mixed for 2 minutes. The resulting suspensions were centrifuged at 2,000 x *g* at 20 °C for 10 minutes, and 50 μL of the supernatant was transferred to a 96-well plate and derivatized using a modified version of the published protocol.[126] An aliquot of the reaction mixture was analyzed by liquid-chromatography mass spectrometry (LC-MS/MS) using an Exion UHPLC (Sciex) coupled to a 5500+ Triple Quadrupole Mass Spectrometer (Sciex) in ESI negative mode using a C18 column (Zorbax Eclipse plus C18 1.8 micron, 2.1x50 mm, Agilent). The peak areas of the respective parent to product ion transitions were measured against the peak area of the parent to product ion transitions of the corresponding labelled internal standards for the quantitated metabolites. Quantitation was performed with Sciex OS-MQ software (Sciex) based on fortified calibration standards prepared immediately prior to each run. Data were normalized to wet weight based on the exact wet weight of each sample, or volume. The lower and upper limits of quantification in intestinal contents were 0.000680 and 121 mmol/kg for propionate, 0.00134 and 104 mmol/kg for lactate, and 0.00102 and 300 mmol/kg for acetate. The lower and upper limits of quantification in culture supernatants were 0.00169 and 83.01 mM for propionate, 0.01665 and 188.2 mM for lactate, and 0.075 and 300 mM for acetate.

QUANTIFICATION AND STATISTICAL ANALYSIS

Unless otherwise noted, statistical analyses were performed using GraphPad Prism version 9.0.2 or higher for Windows, GraphPad Software, San Diego, California USA, www.graphpad.com.

Statistical analyses of whole metagenomic sequencing data were performed using the R(v4.2.0) package *vegan*[124] or the R package *ALDEx2*.[121] Alpha diversity (Shannon diversity and observed reads) and beta diversity (Bray-Curtis dissimilarity) metrics were calculated using the *vegan*[124] and *phyloseq*[120] packages in R (v2.6-2, v1.41.0). PERMANOVA was calculated on Bray-Curtis dissimilarity using the *pairwise Adonis2* package in R[125] and employs a Benjamini-Hochberg correction for multiple comparisons. Distances to centroid were calculated using *phyloseq*[120] and *usedist* (v0.4.0)[123] packages in R and compared across groups using ANOVA. Differential abundance analysis was performed on centered-log-ratio (CLR) transformed data using the ALDEx2 package in R (v1.29.1).[121] Time course analyses employed the repeated measures ANOVA on log transformed data with time and treatment as categorical variables. Time-to-event analysis (Kaplan Meier curve) was run on log transformed data using the *finalfit* package in R (v1.0.5).[122]

p values were adjusted as appropriate. A *p*-value <0.05 was considered significant after adjustment for multiple comparisons where appropriate. Unless otherwise stated, significance values are noted as follows: * $p < 0.05$, ** $p < 0.01$, *** $p < 0.001$, **** $p < 0.0001$.

Figure 2: Significance of differences in *B. infantis* levels were calculated using a mixed effects model for repeated measures with time treated as a categorical variable; significance between kinetic curves was determined using the time versus treatment factor, and significance between groups at individual timepoints was determined using Sidak's post-test for multiple comparisons. For 2A-C, data were log-transformed prior to analysis.

Figure 3A: Significance of differences in Shannon Diversity were calculated using a mixed effects model for repeated measures with time treated as a categorical variable; significance between kinetic curves was determined using the time versus treatment factor, and significance between timepoints across groups was determined using Sidak's post-test for multiple comparisons.

Figures 3B and 3D: Significance of Bray-Curtis dissimilarity between groups was determined using PERMANOVA analysis with Benjamini-Hochberg correction for multiple comparisons.

Figures 3E and 3F: Significance of differences in abundance was determined using Wilcoxon's Rank Sum Test with Benjamini-Hochberg correction for multiple comparisons. Data were CLR transformed prior to analysis.

Figure 4A: Significance of differences in metabolite levels were calculated using a mixed effects model for repeated measures with time treated as a categorical variable; significance between kinetic curves was determined using the time versus treatment factor, and significance between timepoints across groups was determined using Sidak's post-test for multiple comparisons. Data were log-transformed prior to analysis.

Figure 4B: Significance of differences in acetate recovery were calculated using a log rank-test.

Figure 4C: Significance of differences in metabolite levels were calculated using a mixed effects model for repeated measures with time treated as a categorical variable; significance between kinetic curves was determined using the time versus treatment factor, and significance between groups at individual timepoints was determined using Sidak's post-test for multiple comparisons. Data were log-transformed prior to analysis.

Figure 4D: Significance of metabolite changes were calculated by two-way repeated measures ANOVA with Bonferroni 0.05 for multiple comparisons.

Figures 4E and 4F: Significances of differences in fecal metabolites were calculated by two-way repeated measures ANOVA with Bonferroni 0.05 for multiple comparisons. Significance of differences in serum metabolite levels were calculated using a mixed effects model for repeated measures with time treated as a categorical variable; significance between kinetic curves was determined using the time versus treatment factor, and significance between groups at individual timepoints was determined using Sidak's post-test for multiple comparisons. Data were log-transformed prior to analysis.

Figure 5: Significances of differences between treatments were calculated by two-way ANOVA with Tukey's test for multiple comparisons within each *Veillonella* inoculum condition. Data were log-transformed prior to analysis.

Figure 6B: Significance of differences in *Veillonella* levels were calculated using a mixed effects model for repeated measures with time treated as a categorical variable and with two-factor matching; significance between groups at individual timepoints or between timepoints within groups was determined using Sidak's post-test for multiple comparisons. Data were log-transformed prior to analysis.

Figures 6C and 6D: Significance of differences in metabolite levels were calculated using a mixed effects model for repeated measures; significance between groups for each metabolite was determined using Sidak's post-test for multiple comparisons. Data were log-transformed prior to analysis.

Figures S1A–S1D: Significance of differences in *B. infantis* levels were calculated using a mixed effects model for repeated measures with time treated as a categorical variable; significance between kinetic curves was determined using the time versus treatment factor, and significance at individual timepoints was determined using Sidak's post-test for multiple comparisons. For S1A, data were log-transformed prior to analysis.

Figure S1E: Significance of differences in *B. infantis* levels were determined using two-way ANOVA with Sidak's post-test for multiple comparisons.

Figures S2A and S2B: Significance of differences in diversity metrics were calculated using a mixed effects model for repeated measures with time treated as a categorical variable; significance between kinetic curves was determined using the time versus treatment factor, and significance between timepoints across groups was determined using Sidak's post-test for multiple comparisons. For S2B, data were log-transformed prior to analysis.

Figure S2D: Significance of Bray-Curtis dissimilarity between groups was determined using PERMANOVA analysis with Benjamini-Hochberg correction for multiple comparisons.

Figures S2E–S2H: Significances were calculated using Wilcoxon's Rank Sum Test with Benjamini-Hochberg correction for multiple comparisons.

Figures S3A–S3K: Significance of differences in abundance was determined using Wilcoxon's Rank Sum Test with Benjamini-Hochberg correction for multiple comparisons. Data were CLR transformed prior to analysis.

Figure S3L: Correlation and significance were calculated using the repeated measures correlation rmcorr package in R. Data were CLR transformed prior to analysis.

Figures S4A and S4C–S4F: Significance of differences in metabolite levels or pH values were calculated using a mixed effects model for repeated measures with time treated as a categorical variable; significance between kinetic curves was determined using the time versus treatment factor, and significance between timepoints across groups or between groups at individual timepoints was determined using Sidak's post-test for multiple comparisons. For S4A,C,E,F, data were log-transformed prior to analysis.

Figure S4B: Significance of differences in acetate recovery were calculated using a log rank-test.

Figure S4G: Significance of Bray-Curtis dissimilarity between groups were determined using PERMANOVA analysis with Benjamini-Hochberg correction for multiple comparisons.

Figures S4H–S4P: Significance in metabolite changes were calculated by two-way repeated measures ANOVA with Bonferroni 0.05 for multiple comparisons.

Figure S5: Significances of differences in serum metabolite levels were calculated using mixed effects model for repeated measures with time treated as a categorical variable; significance between kinetic curves was determined using the time versus treatment factor, and significance between groups at individual timepoints was determined using Sidak's post-test for multiple comparisons.

Significance of fecal metabolite changes were calculated by two-way repeated measures ANOVA with Bonferroni 0.05 for multiple comparisons.

Figures S6D and S6F: Significances of differences between groups were calculated by two-way ANOVA with Tukey's test for multiple comparisons within each *Veillonella* inoculum condition. Data were log-transformed prior to analysis.

Figures S6E and S6G: Significances of differences between *Veillonella* inoculum conditions were calculated by two-way ANOVA with Tukey's test for multiple comparisons within each treatment. Data were log-transformed prior to analysis.

Figures S6H and S6I: Significances of differences in *Veillonella* or *B. infantis* levels were calculated using a mixed effects model for repeated measures with time treated as a categorical variable; significance between groups at individual timepoints or between time-points within groups was determined using Sidak's post-test for multiple comparisons. Data were log-transformed prior to analysis.

Figure S6J: Significance of differences in acetate levels were calculated using a mixed effects model for repeated measures; significance between groups for each metabolite was determined using Sidak's post-test for multiple comparisons. Data were log-transformed prior to analysis.

Table S1: Significance of differences between the three study arms were evaluated with respect to age and BMI using the 1-way analysis of variance. For the three categorical variables of sex, ethnicity (Hispanic/non-Hispanic), and race (dichotomized to Caucasian versus not), a chi-square test for homogeneity was used.

Table S4: Significance of Bray-Curtis dissimilarity between groups was determined using PERMANOVA analysis with Benjamini-Hochberg correction for multiple comparisons.

Table S6: Significances of differences between treatments were calculated by two-way ANOVA with Tukey's test for multiple comparisons within each *Veillonella* inoculum condition. Data were log-transformed prior to analysis.